CORONAVIRUS

BNT162b2 vaccination induces durable SARS-CoV-2–specific T cells with a stem cell memory phenotype

Gisella Guerrera[1]†, Mario Picozza[1]†, Silvia D'Orso[1], Roberta Placido[1], Marta Pirronello[1], Alice Verdiani[1], Andrea Termine[2], Carlo Fabrizio[2], Flavia Giannessi[1], Manolo Sambucci[1], Maria Pia Balice[3], Carlo Caltagirone[4], Antonino Salvia[5], Angelo Rossini[5], Luca Battistini[1]*, Giovanna Borsellino[1]*

Vaccination against severe acute respiratory syndrome coronavirus 2 (SARS-CoV-2) is effective in preventing hospitalization from severe COVID-19. However, multiple reports of breakthrough infections and of waning antibody titers have raised concerns on the durability of the vaccine, and current vaccination strategies now propose administration of a third dose. Here, we monitored T cell responses to the Spike protein of SARS-CoV-2 in 71 healthy donors vaccinated with two doses of the Pfizer-BioNTech mRNA vaccine (BNT162b2) for up to 6 months after vaccination. We found that vaccination induced the development of a sustained anti-viral CD4$^+$ and CD8$^+$ T cell response. These cells appeared before the development of high antibody titers, displayed markers of immunological maturity and stem cell memory, survived the physiological contraction of the immune response, and persisted for at least 6 months. Collectively, these data show that vaccination with BNT162b2 elicits an immunologically competent and long-lived SARS-CoV-2–specific T cell population.

INTRODUCTION

About half of the world population has developed some immunity to severe acute respiratory syndrome coronavirus 2 (SARS-CoV-2), either through natural infection or through vaccination (*1*), but it is unclear whether this immunity will last long term. SARS-CoV-2 infection elicits a robust immune response (*2*–*10*), as do mRNA vaccines (*11*–*18*), inducing both B and T cell responses. Effective humoral immunity involves the generation of high-affinity neutralizing antibodies, which are widely used as indicators of protective immunity (*19*–*21*) and represent the final output of a coordinated cellular response. The emergence of activated T cells precedes recovery from coronavirus disease 2019 (COVID-19) (*7*, *22*–*24*), providing evidence of T cell involvement in the immune response to SARS-CoV-2. Initial in vitro studies characterized patient-derived antigen-specific CD4$^+$ and CD8$^+$ lymphocytes reactive with overlapping peptide pools from the SARS-CoV-2 Spike protein (*3*, *5*, *23*, *25*), showing the establishment of an effective antiviral response after natural infection. Spike-specific T cells persist in COVID-19 convalescents (*2*, *26*–*28*), arise after vaccination with mRNA-based SARS-CoV-2 vaccines, and include specialized subsets that can both sustain cytotoxic functions and participate to the maturation of antibody-producing B cells in lymph node germinal centers (*11*, *15*–*17*, *29*, *30*). Subjects with undetectable or impaired humoral responses can recover from COVID-19 (*31*–*33*), underlining the importance of cellular immunity in clearing SARS-CoV-2 infection.

Mass vaccination against COVID-19 is effective and protects against severe COVID-19 in real-world settings (*34*, *35*). Decreases of antibody levels and increases of breakthrough infections point to waning immunity of vaccination over time (*36*–*39*). However, despite the decline in antibody levels, protection from severe disease and hospitalization remains high (*40*, *41*), suggesting that persisting cellular immunity drives the immune response and prevents viral dissemination when antibodies disappear. Studies on immune memory to other coronaviruses have shown that cellular immunity can be detected for up to 17 years after initial infection in the absence of antibodies (*9*, *40*–*42*), with cellular immunity persisting for up to 15 months after SARS-CoV-2 infection (*43*). The study of the cellular immune components induced by vaccination and the assessment of their persistence is fundamental; in this respect, a recent study has shown that robust adaptive immune responses can be detected for up to 6 months after mRNA vaccination (*15*).

Here, we performed a longitudinal study looking at the T cell responses and anti–receptor binding domain (RBD) antibodies in 71 health care workers and scientists vaccinated with the BNT162b2 vaccine following the European Medicines Agency (EMA)–approved two-dose vaccination schedule, up to 6 months after the first dose. We investigated expression of phenotypic markers associated with the differentiation, polarization, and cytotoxic functions of Spike-specific T cells and monitored the evolution of the adaptive immune response induced by mRNA vaccination. Vaccination induced the generation of immunologically competent Spike-specific T cells, including potentially long-lived memory stem cells, pilasters of durable immunity. This information provides further information on the durability of the vaccine, which may inform vaccination strategies going forward.

RESULTS

Induction and persistence of anti-RBD antibodies

The antibody response to vaccination with BNT162b2 was measured in serum samples obtained at baseline (T0), on the day of the boost (T1), 14 days later (T2), and 6 months after the first dose (T3). All individuals in our cohort were devoid of anti-RBD antibodies at baseline, and significant levels appeared in 100% of individuals only

[1]Neuroimmunology Unit, Santa Lucia Foundation IRCCS, Rome, Italy. [2]Data Science Unit, Santa Lucia Foundation IRCCS, Rome, Italy. [3]Clinical Microbiology Laboratory, Santa Lucia Foundation IRCCS, Rome, Italy. [4]Department of Clinical and Behavioral Neurology, Santa Lucia Foundation IRCCS, Rome, Italy. [5]Medical Services, Santa Lucia Foundation IRCCS, Rome, Italy.
*Corresponding author. Email: g.borsellino@hsantalucia.it (G.B.); l.battistini@hsantalucia.it (L.B.)
†These authors contributed equally to this work.

after the second dose (fig. S1A) (T1: median 28; T2: median 1786; T3: median 517). Age and sex are key variables in immunity induced by vaccination, whose effectiveness decreases with age and is usually lower in males (*44*). In our cohort, antibody levels induced by BNT162b2 were comparable between males and females (fig. S1B), similar to other studies (*45*). Also, we found that antibody titers negatively correlated with age at all time points, confirming previous results (fig. S1C) (*45*–*47*). Thus, the data show that BNT162b2 induces the production of anti-RBD antibodies, which decrease over time but are maintained at high levels for at least 6 months.

Induction and durability of the Spike-specific T cell response

To investigate the cellular immune response induced by vaccination, we exposed freshly obtained peripheral blood mononuclear cells (PBMCs) to peptide pools spanning the entire sequence of the Spike (S) protein. Blood collection was performed at the same time points as outlined above. To fully capture the antigen-specific T cell response and to maximize sensitivity, two separate assays for the detection of the expression of surface activation-induced markers (AIM) and for intracellular cytokine staining (ICS) were set up (see fig. S2 for gating strategy). All assays were performed on freshly isolated PBMCs to obtain accurate absolute cell counts.

AIM^+ $CD4^+$ T cells were defined by upregulation of CD40L and CD69 (*48*), whereas CD137 and CD69 expression identified the AIM^+ $CD8^+$ subset (*5*) (Fig. 1A). After paired background subtraction from parallel unstimulated cultures, and having set a threshold for positivity at 0.008% for $CD4^+$ T cells and 0.079% for CD8 T cells (see Materials and Methods for further details), we found that 97% of donors had detectable numbers of AIM^+ $CD4^+$ cells at baseline (T0; Fig. 1, B and C, and fig. S3A). Twenty-one days after the first dose of vaccine, these cells were expanded sixfold compared with baseline (T1) and further still at 14 days after the boost (T2). Six months after the first dose (T3), AIM^+ $CD4^+$ cell numbers were still fivefold higher compared with baseline and were detected in all donors. AIM^+ $CD8^+$ T lymphocytes were present at baseline in only 18% of the donors (Fig. 1, B and C, and fig. S3A). After vaccination, 87% showed Spike-specific $CD8^+$ T cells, which had expanded 11-fold from baseline; after further expansion after the second dose, these cells remained detectable after 6 months in 88% of donors (Fig. 1, B and C, and fig. S3A). The total magnitude of the T cell response (including both $CD4^+$ and $CD8^+$ cells) increased significantly after priming (T1) and rechallenge (T2) but decreased 6 months after the first dose (T3) (Fig. 1D and fig. S3B). The stimulation index (S.I.; the ratio of AIM^+ T cells in stimulated over unstimulated samples) was used to determine T cell activation (*49*), and the cutoff for positive responses was arbitrarily set at 3. The S.I. of AIM^+ $CD4^+$ cells increased markedly after the first dose, remained at high levels after boosting, and decreased after 6 months, remaining more than fivefold higher compared with baseline (Fig. 1E). The S.I. of AIM^+ $CD8^+$ T cells peaked 14 days after the boost, and declined by one-third at the latest time point (Fig. 1E). More than 70% of individuals in our cohort showed AIM^+ $CD4^+$ cells with S.I. > 3 already at baseline, and this proportion increased to 100% 6 months after receiving the first dose (Fig. 1F). On the other hand, only 7% of individuals showed AIM^+ $CD8^+$ with S.I. > 3 cells at baseline, with this fraction increasing to 60 and 75% after priming and boosting, and then decreasing to 63% at the latest time points (Fig. 1F). The frequency of S-specific $CD4^+$ (and not $CD8^+$) T cells induced by vaccination inversely correlated with age only at T1, although a tendency toward reduced numbers of activated T cells with increasing age was observed at all time points (fig. S3C), again with no significant differences between males and females (fig. S3D).

In univariate regression, the number of AIM^+ cells correlated with antibody levels only after priming and not at subsequent time points (fig. S3E), suggesting that humoral and cellular immune responses follow different kinetics. Multivariate regression modeling indicated that the number of AIM^+ $CD4^+$ cells 21 days after priming was the best predictor of anti-RBD levels after 6 months, as expected from a T cell–dependent B cell response (Fig. 1G).

Two donors in the cohort presented exceptionally high frequencies of $CD4^+$ and $CD8^+$ AIM^+ cells at baseline (fig. S4A). Vaccination boosted the frequency of AIM^+ cells, but antibody responses remained within the 25th and 75th percentile of the distribution of the whole cohort at all time points (fig. S4B). Thus, vaccination induces detectable and robust antigen-specific T cells that develop before high antibody titers, with most T cell expansion occurring after the first dose and persisting for up to 6 months.

Cytokine production by S-specific T cells

Cytokine production was assessed by ICS after stimulation overnight with the peptide pools in the presence of monensin and brefeldin (Fig. 2A). Measurement of cytokine production showed that, at baseline, 45 and 46% of the tested donors had IFN-γ^+ $CD4^+$ and $CD8^+$ cells, respectively (Fig. 2, B and C). Three weeks after the first dose, 83% of individuals had IFN-γ^+ $CD4^+$ T cells, whereas $CD8^+$ IFN-γ^+ were found in 71% of individuals. Two weeks after the boost, 81 and 68% of individuals had IFN-γ^+ $CD4^+$ and $CD8^+$ T cells, respectively; these cells were maintained for 6 months. Fifty-three percent of donors at baseline showed IL-2^+ $CD4^+$ T cells; this fraction increased to 84% after the first dose then reached 94% after the boost, and remained detectable after 6 months. Polyfunctional IFN-γ^+ IL-2^+ $CD4^+$ T cells were induced in 99% of the individuals only after the booster dose and persisted for at least 6 months after the first dose (Fig. 2D). $CD8^+$ T cells coexpressing IFN-γ^+ and lysosomal associated membrane glycoprotein (CD107a) increased significantly after the boost (Fig. 2D). Induction of cytokine-secreting S-specific T cells was equivalent in both sexes at all time points (fig. S5A). The number of tumor necrosis factor–α (TNFα)–secreting $CD4^+$ and $CD8^+$ cells was highest at the peak of the secondary response, 14 days after the second dose (fig. S5B); at the same time point, polyfunctional TNFα$^+$ IFN-γ^+ cells decreased significantly, and, after 6 months, they were at prevaccination levels. Further analysis of CD107a, TNFα, and granzyme B coexpression among $CD4^+$ and $CD8^+$ T cells producing IFN-γ^+ revealed changing patterns between time points ($P < 0.001$ for all comparisons except for IFN-γ^+ $CD4^+$ T cells between T1 and T2; Fig. 2E), with the fraction of polyfunctional $CD4^+$ cells increasing at each time point, and a predominance of $CD8^+$ cells with two functions at the latest time point, indicating dynamic changes of functional programs in antigen-specific T cells after boost and contraction.

At the peak of the response (T2), cytokine secretion was also measured with a MACSPlex assay in the supernatants of cultures stimulated with the peptide pools for the AIM assays. Production of high levels of interferon-γ (IFN-γ) and interleukin-1 (IL-2) was found, whereas IL-17 and IL-4 were barely detectable (<5 pg/ml), confirming the T helper 1 (T_H1) differentiation profile of S-specific cells (fig. S5C). Thus, vaccination induces the emergence of a robust $CD4^+$ and $CD8^+$ cytokine response by T cells after priming, whereas

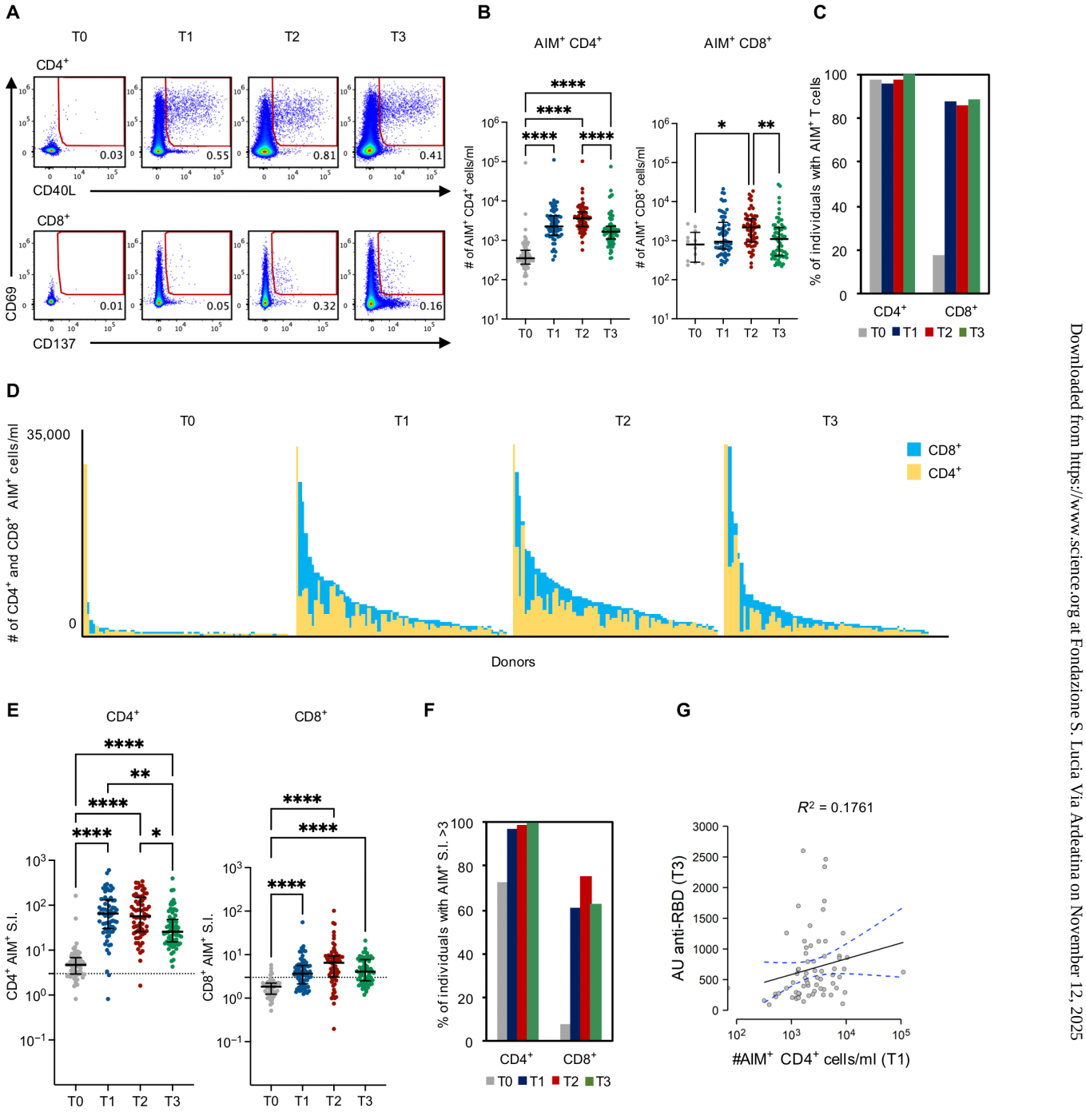

Fig. 1. Spike-specific T cell responses induced by vaccination with BNT162b2. (**A**) Representative flow cytometry plots gated on $CD4^+$ or $CD8^+$ T cells showing upregulation of activation markers (CD69 and CD40L for $CD4^+$ cells and CD69 and CD137 for CD8 cells) following overnight stimulation with a pool of overlapping peptides covering the wild-type Spike protein at baseline (T0), 21 days after the first dose (T1), 14 days after the second dose (T2), and 6 months after initial vaccination (T3). Numbers in gates represent percentages of positive cells. (**B**) Longitudinal analysis of Spike-specific $CD4^+$ and $CD8^+$ absolute cell counts, following background subtraction in paired unstimulated samples. Time points were compared by nonparametric Kruskall-Wallis and Dunn's multiple comparison test; lines represent median with interquartile range. *$P < 0.05$; **$P < 0.01$; ***$P < 0.001$; no symbol, not significant. (**C**) Fraction of individuals showing Spike-specific AIM^+ $CD4^+$ and $CD8^+$ cells above threshold at each time point. (**D**) Magnitude of T cell responses. AIM^+ $CD4^+$ and $CD8^+$ absolute cell counts were aggregated for each donor and displayed in the bar charts at the different time points, ordered by height. (**E**) Stimulation indices (ratio of AIM^+ cells stimulated and paired unstimulated samples) of $CD4^+$ and $CD8^+$ cells in the different time points; time points were compared by nonparametric Kruskall-Wallis followed by Dunn's post hoc tests; bars represent median with interquartile range. *$P < 0.05$; **$P < 0.01$; ***$P < 0.001$; ****$P < 0.0001$; no symbol, not significant. Dotted line indicates S.I. = 3. (**F**) Fraction of individuals showing S.I. > 3 in $CD4^+$ and $CD8^+$ cells at the different time points. (**G**) A linear regression model was fitted to test for T1 significant predictors of T3 anti-RBD antibody serum levels. Variables were $\log_{10}$-scaled when their distribution was not normal. Model's R^2 was 0.18. **$P < 0.01$. The number of AIM^+ $CD4^+$ cells per milliliter was deemed as significant **$P < 0.01$. Continuous and dotted lines represent linear regression and 95% confidence intervals, respectively. AU, Arbitrary Units.

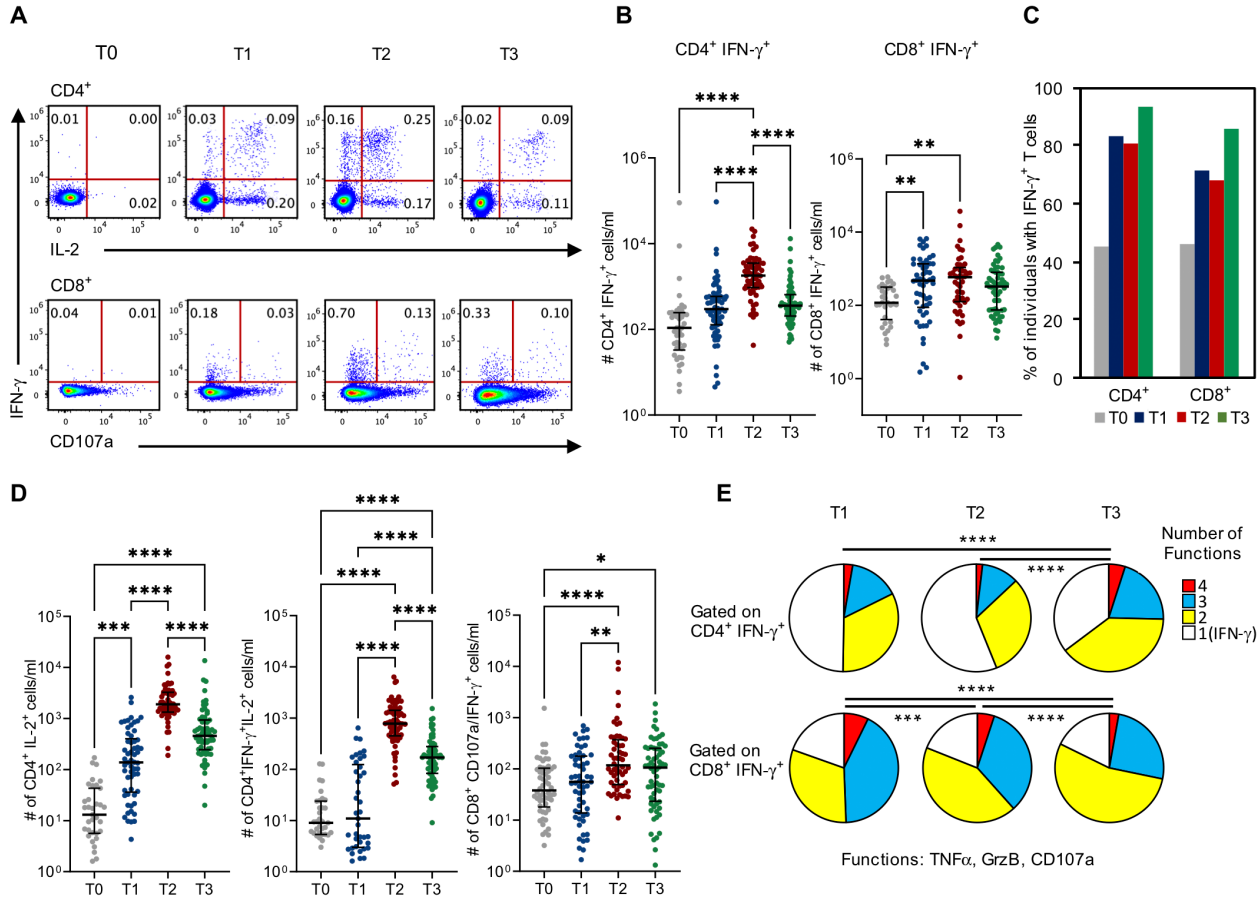

Fig. 2. Spike-specific T cell responses characterized by cytokine production and expression of cytotoxicity markers. (**A**) Representative flow cytometry plots gated on CD4$^+$ or CD8$^+$ T cells showing production of IFN-γ and IL-2 by CD4$^+$ cells (top) and of both IFN-γ production and upregulation of CD107a by CD8$^+$ cells (bottom) following peptide pool stimulation. Numbers in gates indicate percentages of positive cells. (**B**) Longitudinal analysis of absolute cell counts of Spike-specific IFN-γ–producing CD4$^+$ and CD8$^+$ cells. Time points were compared by nonparametric Kruskall-Wallis Dunn's multiple comparison tests; lines represent median with interquartile range. *P < 0.05; **P < 0.01; ***P < 0.001; ****P < 0.0001; no symbol, not significant. (**C**) Fraction of individuals showing Spike-specific IFN-γ$^+$ CD4$^+$ and CD8$^+$ cells at each time point. (**D**) Longitudinal analysis of Spike-specific CD4$^+$ cells producing IL-2 or both IL-2 and IFN-γ (left and center) and of CD8$^+$ cells expressing both CD107a and IFN-γ (left). P values were determined as in (B). (**E**) Coexpression of functional markers [CD107a, granzyme B (Grz B), and TNFα] in IFN-γ–producing S-specific CD4$^+$ and CD8$^+$ T cells. The percentage of T cells positive for the specified number of functions is indicated by the pie slices for each time point, with functions = 1 indicating the fraction of cells that produce only IFN-γ (gating parameter). A partial permutation test (10,000 iterations, Monte Carlo simulation) was applied on distributions into combinatorial gates. ***P < 0.001; ****P < 0.0001.

full effector functions marked by polyfunctionality are acquired after the boost, and then maintained for at least 6 months.

Differentiation features of Spike-specific T cells

We then characterized the antigen-specific T cells induced by vaccination through the definition of their differentiation status using CCR7 and CD45RA markers to define naïve (N), central memory (CM), effector memory (EM), and terminally differentiated effector (EMRA) populations (Fig. 3, A and B, and fig. S2). The study of the frequencies of these subsets within AIM$^+$ cells in the peripheral blood showed that, at all time points, EM cells dominate the CD4$^+$ T cell subset, whereas CD8$^+$ T cells also present a large proportion of terminally differentiated cells (Fig. 3, A and B). Six months after the first dose, CD4$^+$ S-specific cells that had survived the physiological contraction of the immune response were mostly CM and EM cells, whereas, in the CD8$^+$ subset, these cells also included a significant fraction of terminally differentiated effectors (Fig. 3, A and B).

Among the desirable outcomes of vaccination lies the generation of a pool of memory stem cells, which can rapidly and efficiently differentiate in highly effective and polyfunctional lymphocytes in case of re-encounter with their nominal antigen (*50*). Stemness includes long-term persistence, a key aspect in this age of pandemics and uncertainties on the durability of the novel vaccines. Thus, we searched for these cells within the antigen-responsive CD4$^+$ and CD8$^+$ subsets. After the first dose, CD4$^+$AIM$^+$CD45RA$^+$CD27$^+$CCR7^{high}CD95$^+$ cells, representing CD4$^+$ T_{SCM} (T stem cell memory) cells (*51*), were detectable in 88% of individuals (see fig. S6 for gating strategy); 2 weeks after the second dose, this fraction was still 88%; after 6 months, 91% of individuals showed these cells (Fig. 3C). CD8$^+$ T_{SCM} followed similar kinetics, with 94, 87, and 96% of individuals showing these cells at T1, T2, and T3, respectively.

To investigate the possible impact of T_{SCM} on future immune responses, we used a general linear model with stepwise selection aiming to optimize Akaike information criterion with leave-one-out

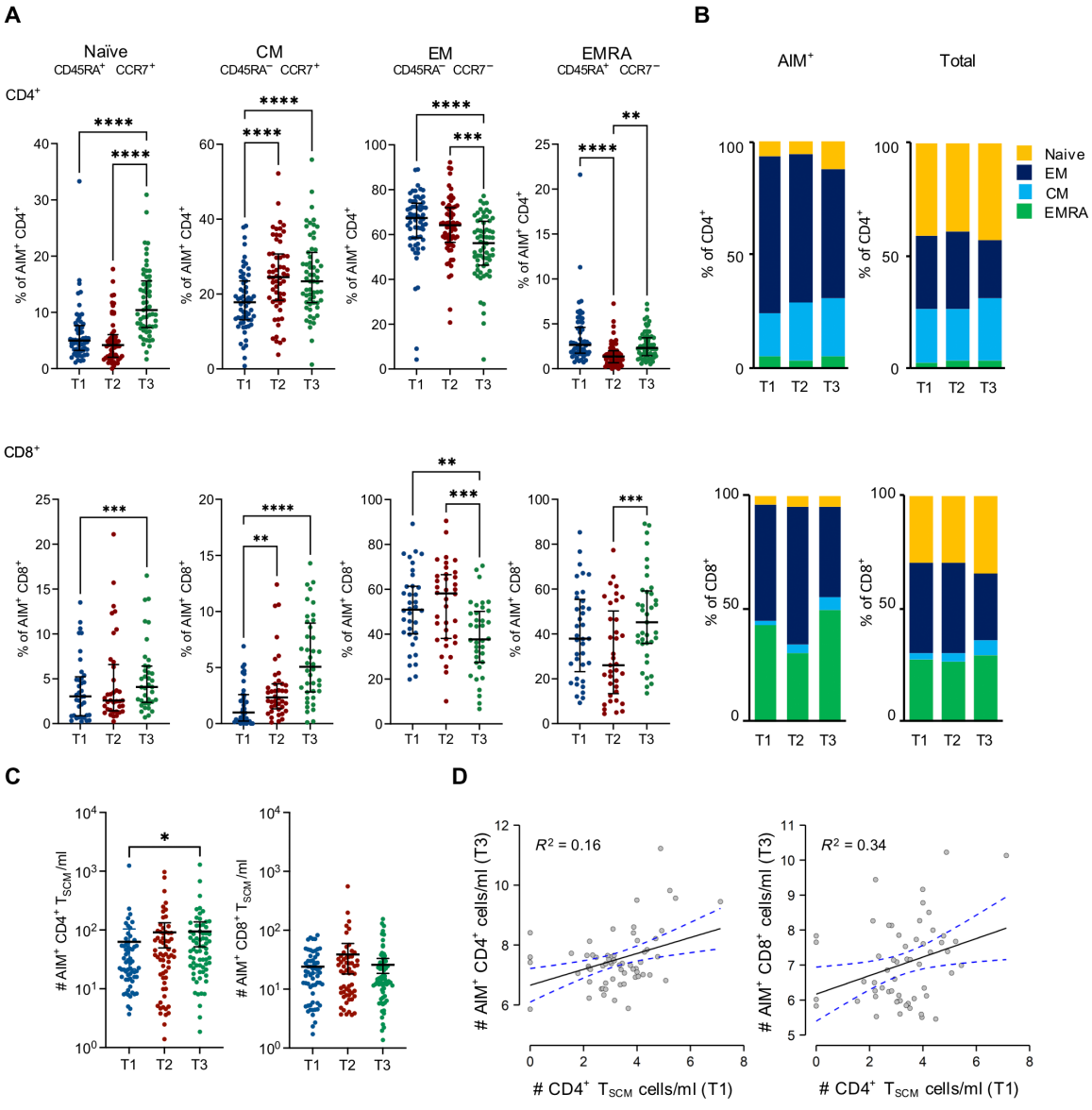

Fig. 3. Differentiation status of Spike-specific CD4$^+$ and CD8$^+$ T cells. (**A**) Frequency of naïve, CM, EM, and CD45RA$^+$ effector memory (EMRA) within AIM$^+$ CD4$^+$ (top) and CD8$^+$ (bottom), at each time point. Time points were compared by nonparametric repeated measures Friedman and Dunn's multiple comparison tests; lines represent median with interquartile range. *P < 0.05; **P < 0.01; ***P < 0.001; ****P < 0.0001; no symbol, not significant. (**B**) Fraction of AIM$^+$ or total CD4$^+$ (top) and CD8$^+$ (bottom) that belong to the indicated subsets at each time point. (**C**) Absolute cell counts of CCR7$^+$CD45RA$^+$CD27$^+$CD95$^+$ AIM$^+$ CD4$^+$ (left) and CD8$^+$ (right) cells at the different time points. Time points were compared by nonparametric Kruskall-Wallis test; lines represent median with interquartile range. *P < 0.05; no symbol, not significant. (**D**) The relevance of T1 CD4$^+$ T_{SCM} cells per milliliter in predicting T3 AIM$^+$ CD4$^+$ (top) and CD8$^+$ (bottom) cells per milliliter was tested with two generalized linear models with stepwise selection aiming to optimize Akaike information criterion. Model's R^2 was 0.16 and 0.34 for AIM$^+$ CD4$^+$ and CD8$^+$ cells, respectively. The number of CD4$^+$ T_{SCM} in T1 cells per milliliter was deemed as significant in predicting both CD4$^+$ and CD8$^+$ AIM$^+$ cell numbers in T3 (*P < 0.05). Continuous and dotted lines represent linear regression and 95% confidence intervals, respectively.

cross-validation. We tested if the number of early (i.e., T1) CD4$^+$ T_{SCM} induced by vaccination significantly predicted immunological outcomes at future time points. We found that the number of T_{SCM} induced after priming was a significant predictor of the number of both CD4$^+$- and CD8$^+$-activated T cells at the latest time point (Fig. 3D). To exclude the possibility that outliers were present in the CD4$^+$ T_{SCM} distribution, we performed multiple Grubbs and Rosner tests and no outliers were found (tables S1 and S2). These findings show that vaccination with BNT162b2 induces a T cell population with features of longevity, which remain numerically stable in the peripheral blood for at least 6 months and predict future T cell responses.

Effector features of Spike-specific CD4$^+$ and CD8$^+$ cells

We next explored the phenotypic changes occurring in AIM$^+$ T cells after boosting and 6 months thereafter by unbiased computational analysis. We used FlowSOM clustering to identify four CD4$^+$ T cell clusters segregated by the expression pattern of CD137, CD39, Inducible costimulator (ICOS), programmed cell death protein 1 (PD-1), Human

leukocyte antigen -DR (HLA-DR), CD25, CXCR5, CD95, CCR7, CD45RA, CD38, and CD127 (table S3) and superimposed those clusters in a Uniform Manifold Approximation and Projection (UMAP) plot generated by embedding the same set of markers (Fig. 4A). AIM^+ $CD4^+$ T cells were distributed differently in the UMAP plot at the three different time points (Fig. 4B), highlighting an overall phenotypic shift. Among these cell clusters, clusters 3 and 4 were unchanged in frequency, whereas clusters 1 and 2 showed significant changes over time (Fig. 4C). Cluster 2 increased in frequency at each time point and was characterized by high expression of activation markers (CD25, CD38, CD39, HLA-DR, and CD137) and of the typical markers of T follicular helper (T_{fh}) cells (i.e., expression of ICOS, PD-1, and CXCR5; Fig. 4, A and C). Cluster 1 was composed of cells that showed the lowest expression of CD25, CD38, CD39, HLA-DR, and CD1379, corresponding to a nonactivated profile, and decreased with time (Fig. 4, A and C).

Data analysis through manual gating and measurement of single-marker expression on the antigen-specific T cells revealed the emergence and persistence in time, albeit at lower levels after 6 months, of $CD4^+$ subsets displaying PD-1, ICOS, and CXCR5 (fig. S7), typical T_{fh} markers. At the 6-month time point, expression of activation markers such as CD25, CD39, CD38, and HLA-DR was greatly reduced. Linear regression modeling indicated that the fraction of $PD\text{-}1^+ICOS^+$ within $CD4^+$ AIM^+ T cells was a significant predictor of antibody levels at the 6-month time point (fig. S8).

S-specific $CD8^+$ lymphocytes were remodeled by vaccine doses, as shown by the distinct distribution with time along the UMAP axes (Fig. 4E). Two clusters, comprising highly (cluster 4) and slightly less (cluster 3) activated AIM^+ $CD8^+$ T cells, showed transient expansion after the booster dose (Fig. 4, D and F). This was in contrast to cluster 1 (naïve-like cells), which remained stable after a decrease in frequency at T2, and to cluster 2 ($CCR7^+CD127^+CD45RA^-$ CM $CD8^+$ T cells), which was not significantly reduced at T2 but increased in size at 6 months. Manual analysis of AIM^+ $CD8^+$ T cells confirmed the transient increase at T2 of $CD38^+$, $HLA\text{-}DR^+$, and $CD25^+$ cell frequencies, whereas $CD39^+$ and $PD\text{-}1^+$ cells steadily decreased or increased, respectively, at T2 and T3 compared with T1 (fig. S7). Thus, antigen-specific T cells acquire phenotypic features of activation and functional capability after the booster, and most of these attributes are less evident and partially replaced, in the long run, by characteristics distinctive of more quiescent memory cells.

DISCUSSION

Multiple different vaccines are being administered globally to prevent the infection and spread of SARS-CoV-2. Here, we studied the adaptive immune response induced by vaccination with BNT162b2 to characterize Spike-specific T cell responses and to understand whether vaccine-induced T cells displayed features of longevity. We found Spike-specific $CD4^+$ and $CD8^+$ memory T cells that peaked 2 weeks after the boost and remained detectable in the peripheral blood for up to 6 months. These findings are in line with those of Goel *et al.* (*15*), who have recently described the establishment and durability of memory T cells after mRNA vaccination, and with previous studies investigating cellular immunity after SARS-CoV2 infection (*2*, *26*, *28*). Also, we found antigen-specific population of T_{SCM}, which persisted overtime.

In our cohort, nearly all individuals harbored Spike-specific T cells at baseline, likely due to the presence of a pool of memory clones cross-reactive with other coronaviruses. Preexisting T cell cross-reactivity to endemic coronaviruses, such as common cold coronaviruses, has been described in various proportions of SARS-CoV-2–naïve individuals (*5*, *9*, *23*, *24*, *49*, *52*–*54*). Bacher *et al.* (*54*), using freshly isolated cells, detected Spike-specific T cells in all tested donors, similar to our findings. The presence of SARS-CoV-2 cross-reactive T cells associates with an enhanced cellular and humoral response to vaccination (*49*). The individuals in our cohort with exceptionally high numbers of AIM^+ $CD4^+$ cells at baseline did not respond to vaccination with an equally exceptional antibody response. This could be due to the fact that cross-reactive T cells mainly target the S-II region of the Spike protein (*49*), which does not contain the RBD-binding region; thus, measurement of only anti-RBD antibodies may not inform on the whole spectrum of the humoral response induced by vaccination.

An optimal antibody response is the consequence of a competent underlying T cell response, which relies on the presence of T_{fh} cells that interact with B lymphocytes in germinal centers to promote high-affinity antibody production and the generation of long-lived memory B cells (*55*). High antibody titers induced by influenza vaccination positively correlate with the frequency of T cells expressing follicular helper molecules, including CXCR5 and ICOS (*56*, *57*). Induction of T_{fh} cells also occurs in response to the Spike protein (*58*, *59*), and our finding of Spike-specific cells expressing CXCR5, PD-1, and ICOS suggests that mRNA vaccination is effective in generating $CD4^+$ cells able to interact with B cells, in line with other studies (*13*, *15*, *17*, *60*). Accordingly, the simultaneous measurement of serum levels of anti-RBD antibodies showed the effective induction of the humoral arm of the adaptive response in all individuals in our cohort. Although antibody titers did decline with time, they were maintained at high levels for the entire period of our observation. Our data also converge with a recent study showing that the magnitude of antigen-specific CD4 responses at early time points predicted antibody levels after 6 months, confirming the central role of $CD4^+$ T cells in instructing the humoral response (*15*).

$CD4^+$ T cells also sustain immune responses through the production of cytokines, and we find that mRNA vaccination elicits a vigorous T_H1-skewed response, with production of IFN-γ, IL-2, and TNFα by Spike-specific cells, and undetectable levels of IL-4 and IL-17. After 6 months, T cell responses were maintained, with the persistence of a numerically consistent pool of polyfunctional memory antigen-specific T cells (*61*). A correlation between both magnitude and polyfunctionality of T cell responses and resistance to infection or favorable disease evolution has been described in successful vaccine settings (*62*–*68*), and polyfunctional T cells correlate to protection against influenza (*69*). Polyfunctional cells were also detected in the $CD8^+$ Spike-specific T cell subset, which produced IFN-γ and TNFα and expressed granzyme B and the surrogate marker of degranulation CD107a, in agreement with previous studies (*12*, *15*, *17*, *70*, *71*). $CD8^+$ T cells, however, were less expanded compared with the $CD4^+$ subset and showed lower S.I., probably due to the fact that the peptide pool used in this study, consisting of 15-mers, is not optimal for presentation through major histocompatibility complex I and thus for $CD8^+$ T cell recognition (*72*), so these responses might have been underestimated.

We found that mRNA vaccination also induced $CD4^+$ and $CD8^+$ T_{SCM}, which were stable throughout the 6-month period of this study. T_{SCM} cells provide a memory reservoir with multipotent capacity and have been shown to persist for decades (*73*–*76*). The

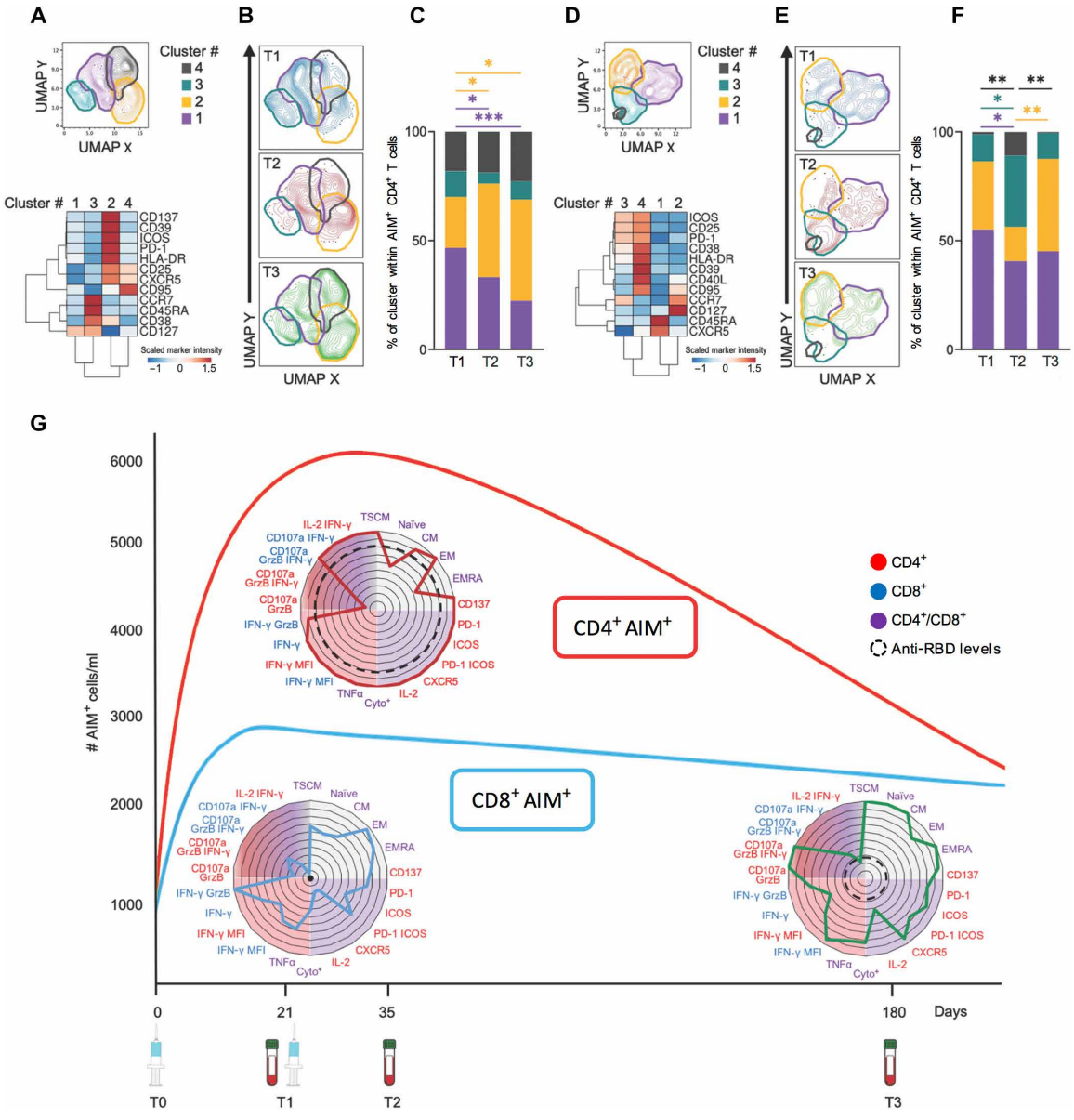

Fig. 4. Phenotypic shifts of AIM$^+$ T cells over time. (**A**) Top: UMAP embedding and FlowSOM clustering based on the expression of the indicated markers on AIM$^+$ CD4$^+$ T cells. The cell clusters identified by FlowSOM were superimposed on the UMAP plots and manually contoured to highlight cluster boundaries. Bottom: Heatmaps with two-way hierachical clustering of scaled and centered median fluorescence intensity values for the indicated markers expressed by the AIM$^+$ CD4$^+$ T cell clusters. (**B**) UMAP plots with AIM$^+$ CD4$^+$ T cells selected from each time point. (**C**) Bar plots showing relative frequency of cell clusters at indicated time points among AIM$^+$ CD4$^+$ T cells. (**D**) Top: UMAP embedding and FlowSOM clustering based on the expression of the indicated markers on AIM$^+$ CD8$^+$ T cells. The cell clusters identified by FlowSOM were superimposed on the UMAP plots and manually contoured to highlight cluster boundaries. Bottom: Heatmaps with two-way hierachical clustering of scaled and centered median fluorescence intensity values for the indicated markers expressed by the AIM$^+$ CD8$^+$ T cell clusters. (**E**) UMAP plots with AIM$^+$ CD8$^+$ T cells selected from each time point. (**F**) Bar plots showing relative frequency of cell clusters at indicated time points among AIM$^+$ CD8$^+$ T cells. Statistical significance was assessed by Friedman test followed by post hoc two-stage linear step-up procedure of Benjamini, Krieger, and Yekutieli. *P < 0.05; **P < 0.01; ***P < 0.001. (**G**) T cell marker measurements from both CD4$^+$ and CD8$^+$ AIM$^+$ cells were normalized across the three time points, and the relative positivity for each marker is displayed on the radar plots. Measurements from CD4$^+$ T cells are shown in red, those from CD8$^+$ cells are blue, and cumulative measurements from both subsets are purple. The resulting plots illustrate the main features of T cells responding to a pool of peptides derived from the Spike protein of SARS-CoV-2. Dashed circles indicate neutralizing anti-Spike antibody levels. Histograms represent CD4$^+$ (red) and CD8$^+$ (blue) cell counts along the timeline. Syringes indicate the time point of vaccine administration, and tubes correspond to the day of blood sampling. Cyto$^+$: aggregation of absolute numbers of CD4$^+$ and CD8$^+$ cell producing at least one cytokine among IFN-γ, IL-2, and TNFα; IFN-γ MFI: mean fluorescence intensity of the IFN-γ signal in IFN-γ$^+$ CD8$^+$ (blue) or CD4$^+$ (red) cells.

detection of TSCM in vaccinated individuals is thus suggestive of the establishment of long-lived immunity. The number of T_{SCM} induced after priming predicted future T cell responses, and the stability of this memory population may point in the direction of durable immunity against SARS-CoV2.

Last, immune responses to vaccines have been shown to be higher in females (*44*, *77*). Moreover, the male sex is associated with severe COVID-19 and death (*78*). Thus, we searched for a sex bias in the immunological parameters investigated. We did not find differences in vaccine-induced immune responses between males and females.

This study has the inevitable limits of human studies, consisting mainly of the wide genetic and immunological variability of the study population, and with blood being the only available source of material. Thus, we only studied circulating lymphocytes, which may be different from those who reside at mucosal barriers and which confer immediate protection against infection. Also, we did not investigate Spike-specific B lymphocytes, and dosage of antibody titers was the only readout of successful induction of humoral immunity. T_{fh} and T_{SCM} cells were identified only by the phenotypic characterization of surface markers, and functional studies, such as measurement of IL-21 production to identify T_{fh} cells, were not carried out to match the phenotype. Further time points will be necessary to measure effective durability of anti–SARS-CoV-2 immune responses. Moreover, although donors were equally distributed for age and sex, our sample was limited in size.

On the whole, the results of this study can be visualized as the dynamic and integrated emergence of a Spike-specific adaptive immune response, characterized by a T cell response that precedes the development of high levels of anti-RBD antibodies (Fig. 4G). T cells induced after the first encounter with the Spike protein are mostly effector cells, which secrete intermediate levels of cytokines, express the highest levels of granzyme B, are not polyfunctional, and only some have T_{fh} characteristics; cells with features of stemness and longevity also appear. After the boost, the peak of the response shows a fully activated, cytotoxically empowered, multifunctional T cell population, including cells of the T_{fh} phenotype; at this time point, the highest levels of anti-RBD antibodies are detected in the serum. What remains after 6 months is a population of T cells with features of polyfunctionality and markers of T_{fh} cells; at this time point, Spike-specific T cells that have survived the immunological contraction are highly specific and theoretically prone to give rise to effective and rapid antiviral responses, both by possibly sustaining the production of antibodies and by exerting cytotoxicity toward already infected cells; concomitantly, the pool of T_{SCM} is stably maintained. This is in line with clinical real-world data showing that vaccine effectiveness in preventing severe COVID-19 is maintained above 90% at least for 6 months (*79*–*81*). Protection from infection, however, does significantly decrease with time and likely correlates to the weaning antibody titers (*21*, *38*), which provide an immediate shield against infection.

Cellular responses to mRNA vaccination thus include richly heterogeneous and dynamic memory T cell populations showing features associated with protective immunity. Previous studies performed at early time points after vaccination have described the induction of memory T_H1 and T_{fh} $CD4^+$ T cells along with cytotoxic $CD8^+$ T cells (*13*, *16*, *17*, *82*, *83*). Observations at more distant time points (6 months) have shown stability of SARS-CoV-2 memory T cells, with a faster decline of the $CD8^+$ subset (*15*). Another study found equivalent levels of $CD4^+$ and $CD8^+$ cells 6 months after vaccination, as observed after natural infection (*13*). Here, we have shown that a sizable population of T_{SCM} is promptly induced by vaccination, but whether these memory progenitors will provide added protection upon viral exposure remains to be established.

MATERIALS AND METHODS

Study design

This work started to define cellular immune responses against the SARS-CoV-2 Spike-protein induced by mRNA vaccine administration. To this aim, we enrolled 71 individuals from health care workers and scientists operating at the Santa Lucia Foundation scheduled for vaccination with Pfizer-BioNTech BNT162b2 between 12 January and 2 February 2021 (table S4). All donors signed informed consent forms approved by the Ethical Committee of the Santa Lucia Foundation. Venous blood was obtained immediately before the first dose (T0), 21 days thereafter, at the time of boosting (T1), two weeks after the second dose (T2), and 6 months after the first dose (T3). The use of freshly obtained blood cells permitted the detection of fragile markers, avoided the bias introduced by freezing/thawing procedures, and provided the possibility to precisely calculate absolute cell counts, a measure routinely used to guide clinical decisions in infectious diseases, such as HIV infection (*84*).

Evaluation of anti–SARS-CoV-2 antibodies

The measurement of anti-RBD antibodies was performed by electrochemiluminescence sandwich immunoassay through Roche Elecsys Anti–SARS-CoV-2 S (Roche Diagnostics, Switzerland). Antibody levels were measured on a Cobas 601 modular analyzer (Roche diagnostics, Switzerland), using a cutoff of 0.8 U/ml. Elecsys Anti-SARS-CoV-2 S U/ml measurements are equivalent to World Health Organization International Standard Binding Arbitrary Units per milliliter (BAU/ml).

AIM assay

In vitro stimulation of freshly obtained PBMCs was performed as previously described (*85*). Briefly, 200 μl of cell suspension (10×10^6 cells/ml) was seeded in U-bottom 96-well plates and stimulated for 18 hours with PepTivator SARS-CoV-2 protein S, S1, and S+ peptide pools (1 mg/ml each; Miltenyi Biotec) or with an equal volume of water. Purified αCD40 (0.5 μg/μl; Miltenyi Biotec) was added at culture start. Supernatants and cells from these culture wells were collected for cytokine measurement and flow cytometry, respectively. The threshold for positivity for background-subtracted values was set using the median 75th percentile of values obtained in negative control cultures (*86*).

Intracellular cytokine staining

PBMCs were incubated with peptide pools or water for 1 hour and then BV421-conjugated antiCD107a (1:200 dilution; BD Biosciences), monensin, and brefeldin A (5 μM and 10 μg/ml, respectively; both from Sigma-Aldrich) were added to the cultures. After an additional 17 hours, cells were harvested and directly stained for flow cytometry.

Flow cytometry staining and acquisition

Postculture cells were pelleted in V-bottom 96-well plates and resuspended in 30 μl of antibodies at preoptimized concentrations and diluted in Brilliant Stain Buffer (BD Biosciences), then incubated

for 15 min at room temperature (RT). Cell pellets were fixed either in FoxP3 fixation/permeabilization buffer (Thermo Fisher Scientific) for 20 min at RT (AIM assay) or in 4% formaldehyde in phosphate-buffered saline (ICS assay). ICS was performed by incubating cells in 30 µl of antibodies against cytokines and granzyme B diluted in a saponin (Sigma-Aldrich) 0.5% w/v solution. The complete list of antibodies used for surface and intracellular staining is shown in tables S5 and S6, respectively. Samples were acquired on a fully equipped CytoFLEX LX within 6 hours from staining and fixation. Quality control beads (Beckman Coulter) were used daily to check and standardize instrument performances. Absolute counts were obtained by a volumetric, lyse-no-wash, flow cytometry approach. Briefly, whole blood was stained (table S7). After 15 min of incubation at RT, fluorescence-activated cell sorting lysing solution (BD Biosciences) was added. After complete red blood cell lysis, samples run on a CytoFLEX with a volume-calibrated peristaltic pump. The number of cells per milliliter automatically derived by the instrument was then multiplied by 10,000 to determine the absolute CD4 and CD8 T cells on a milliliter basis. Absolute counts of AIM^+, $cytokine^+$, and related subsets were then performed multiplying their proportions by the absolute count of parent lineages. Data were analyzed with FlowJo v.10.7. UMAP embedding and FlowSOM clustering of AIM^+ cells were performed with FlowJo (UMAP ver3.1 and FlowSOM ver2.6 plugins). A total of 2500 CD4 and 990 CD8 AIM^+ T cells, equally sampled from 10 donors per three time points, were used to run each algorithm.

Cytokine measurements

IL-4, IL-17, TNFα, and IFN-γ were measured in frozen culture supernatants from the AIM assays described above by a bead-based sandwich enzyme-linked immunosorbent assay (MACSPlex Cytokine Kit, Miltenyi Biotec) according to the manufacturer's instructions.

Statistical analysis

Statistical analyses were performed with GraphPad Prism 9, Spice 6.1, and R programming language using the following libraries: caret 6.0, FactoMineR 2.4, and factoextra 1.0.7. Details of the statistical tests applied for each experiment are illustrated in the respective figure. Time points were compared by Kruskall-Wallis or Friedman test followed by post hoc Dunn's or two-stage linear step-up procedure of Benjamini, Krieger, and Yekutieli. Statistical significance was inferred if $P < 0.05$. In all figures, P values are indicated by $*P < 0.05$; $**P < 0.01$; $***P < 0.001$; $****P < 0.0001$. Outlier detection was performed with multiple Grubbs' test and Rosner's test using the outliers and EnvStats packages in R, respectively.

SUPPLEMENTARY MATERIALS

www.science.org/doi/10.1126/sciimmunol.abl5344
Figs. S1 to S8
Tables S1 to S7
Raw Data

View/request a protocol for this paper from *Bio-protocol*.

REFERENCES AND NOTES

1. WHO Coronavirus (COVID-19) Dashboard; https://covid19/who/int/.
2. J. M. Dan, J. Mateus, Y. Kato, K. M. Hastie, E. D. Yu, C. E. Faliti, A. Grifoni, S. I. Ramirez, S. Haupt, A. Frazier, C. Nakao, V. Rayaprolu, S. A. Rawlings, B. Peters, F. Krammer, V. Simon, E. O. Saphire, D. M. Smith, D. Weiskopf, A. Sette, S. Crotty, Immunological memory to SARS-CoV-2 assessed for up to 8 months after infection. *Science* **371**, eabf4063 (2021).
3. C. R. Moderbacher, S. I. Ramirez, J. M. Dan, A. Grifoni, K. M. Hastie, D. Weiskopf, S. Belanger, R. K. Abbott, C. Kim, J. Choi, Y. Kato, E. G. Crotty, C. Kim, S. A. Rawlings, J. Mateus, L. P. V. Tse, A. Frazier, R. Baric, B. Peters, J. Greenbaum, E. O. Saphire, D. M. Smith, A. Sette, S. Crotty, Antigen-specific adaptive immunity to SARS-CoV-2 in acute COVID-19 and associations with age and disease severity. *Cell* **183**, 996–1012.e19 (2020).
4. A. Sette, S. Crotty, Adaptive immunity to SARS-CoV-2 and COVID-19. *Cell* **184**, 861–880 (2021).
5. A. Grifoni, D. Weiskopf, S. I. Ramirez, J. Mateus, J. M. Dan, C. R. Moderbacher, S. A. Rawlings, A. Sutherland, L. Premkumar, R. S. Jadi, D. Marrama, A. M. de Silva, A. Frazier, A. Carlin, J. A. Greenbaum, B. Peters, F. Krammer, D. M. Smith, S. Crotty, A. Sette, Targets of T cell responses to SARS-CoV-2 coronavirus in humans with COVID-19 disease and unexposed individuals. *Cell* **181**, 1489–1501.e15 (2020).
6. J. Zuo, A. C. Dowell, H. Pearce, K. Verma, H. M. Long, J. Begum, F. Aiano, Z. Amin-Chowdhury, B. Hallis, L. Stapley, R. Borrow, E. Linley, S. Ahmad, B. Parker, A. Horsley, G. Amirthalingam, K. Brown, M. E. Ramsay, S. Ladhani, P. Moss, Robust SARS-CoV-2-specific T cell immunity is maintained at 6 months following primary infection. *Nat. Immunol.* **22**, 620–626 (2021).
7. L. Ni, F. Ye, M.-L. Cheng, Y. Feng, Y.-Q. Deng, H. Zhao, P. Wei, J. Ge, M. Gou, X. Li, L. Sun, T. Cao, P. Wang, C. Zhou, R. Zhang, P. Liang, H. Guo, X. Wang, C.-F. Qin, F. Chen, C. Dong, Detection of SARS-CoV-2-specific humoral and cellular immunity in COVID-19 convalescent individuals. *Immunity* **52**, 971–977.e3 (2020).
8. N. Le Bert, H. E. Clapham, A. T. Tan, W. N. Chia, C. Y. L. Tham, J. M. Lim, K. Kunasegaran, L. W. L. Tan, C.-A. Dutertre, N. Shankar, J. M. E. Lim, L. J. Sun, M. Zahari, Z. M. Tun, V. Kumar, B. L. Lim, S. H. Lim, A. Chia, Y.-J. Tan, P. A. Tambyah, S. Kalimuddin, D. Lye, J. G. H. Low, L.-F. Wang, W. Y. Wan, L. Y. Hsu, A. Bertoletti, C. C. Tam, Highly functional virus-specific cellular immune response in asymptomatic SARS-CoV-2 infection. *J. Exp. Med.* **218**, e20202617 (2021).
9. N. Le Bert, A. T. Tan, K. Kunasegaran, C. Y. L. Tham, M. Hafezi, A. Chia, M. H. Y. Chng, M. Lin, N. Tan, M. Linster, W. N. Chia, M. I.-C. Chen, L.-F. Wang, E. E. Ooi, S. Kalimuddin, P. A. Tambyah, J. G.-H. Low, Y.-J. Tan, A. Bertoletti, SARS-CoV-2-specific T cell immunity in cases of COVID-19 and SARS, and uninfected controls. *Nature* **584**, 457–462 (2020).
10. A. G. Laing, A. Lorenc, I. del Molino del Barrio, A. Das, M. Fish, L. Monin, M. Muñoz-Ruiz, D. R. McKenzie, T. S. Hayday, I. Francos-Quijorna, S. Kamdar, M. Joseph, D. Davies, R. Davis, A. Jennings, I. Zlatareva, P. Vantourout, Y. Wu, V. Sofra, F. Cano, M. Greco, E. Theodoridis, J. Freedman, S. Gee, J. N. E. Chan, S. Ryan, E. Bugallo-Blanco, P. Peterson, K. Kisand, L. Haljasmägi, L. Chadli, P. Moingeon, L. Martinez, B. Merrick, K. Bisnauthsing, K. Brooks, M. A. A. Ibrahim, J. Mason, F. L. Gomez, K. Babalola, S. Abdul-Jawad, J. Cason, C. Mant, J. Seow, C. Graham, K. J. Doores, F. D. Rosa, J. Edgeworth, M. Shankar-Hari, A. C. Hayday, A dynamic COVID-19 immune signature includes associations with poor prognosis. *Nat. Med.* **26**, 1623–1635 (2020).
11. U. Sahin, A. Muik, I. Vogler, E. Derhovanessian, L. M. Kranz, M. Vormehr, J. Quandt, N. Bidmon, A. Ulges, A. Baum, K. E. Pascal, D. Maurus, S. Brachtendorf, V. Lörks, J. Sikorski, P. Koch, R. Hilker, D. Becker, A.-K. Eller, J. Grützner, M. Tonigold, C. Boesler, C. Rosenbaum, L. Heesen, M.-C. Kühnle, A. Poran, J. Z. Dong, U. Luxemburger, A. Kemmer-Brück, D. Langer, M. Bexon, S. Bolte, T. Palanche, A. Schultz, S. Baumann, A. J. Mahiny, G. Boros, J. Reinholz, G. T. Szabó, K. Karikó, P.-Y. Shi, C. Fontes-Garfias, J. L. Perez, M. Cutler, D. Cooper, C. A. Kyratsous, P. R. Dormitzer, K. U. Jansen, Ö. Türeci, BNT162b2 vaccine induces neutralizing antibodies and poly-specific T cells in humans. *Nature* **595**, 572–577 (2021).
12. U. Sahin, A. Muik, E. Derhovanessian, I. Vogler, L. M. Kranz, M. Vormehr, A. Baum, K. Pascal, J. Quandt, D. Maurus, S. Brachtendorf, V. Lörks, J. Sikorski, R. Hilker, D. Becker, A.-K. Eller, J. Grützner, C. Boesler, C. Rosenbaum, M.-C. Kühnle, U. Luxemburger, A. Kemmer-Brück, D. Langer, M. Bexon, S. Bolte, K. Karikó, T. Palanche, B. Fischer, A. Schultz, P.-Y. Shi, C. Fontes-Garfias, J. L. Perez, K. A. Swanson, J. Loschko, I. L. Scully, M. Cutler, W. Kalina, C. A. Kyratsous, D. Cooper, P. R. Dormitzer, K. U. Jansen, Ö. Türeci, COVID-19 vaccine BNT162b1 elicits human antibody and T_H1 T cell responses. *Nature* **586**, 594–599 (2020).
13. J. Mateus, J. M. Dan, Z. Zhang, C. R. Moderbacher, M. Lammers, B. Goodwin, A. Sette, S. Crotty, D. Weiskopf, Low-dose mRNA-1273 COVID-19 vaccine generates durable memory enhanced by cross-reactive T cells. *Science* **374**, eabj9853 (2021).
14. Z. Wang, F. Schmidt, Y. Weisblum, F. Muecksch, C. O. Barnes, S. Finkin, D. Schaefer-Babajew, M. Cipolla, C. Gaebler, J. A. Lieberman, T. Y. Oliveira, Z. Yang, M. E. Abernathy, K. E. Huey-Tubman, A. Hurley, M. Turroja, K. A. West, K. Gordon, K. G. Millard, V. Ramos, J. D. Silva, J. Xu, R. A. Colbert, R. Patel, J. Dizon, C. Unson-O'Brien, I. Shimeliovich, A. Gazumyan, M. Caskey, P. J. Bjorkman, R. Casellas, T. Hatziioannou, P. D. Bieniasz, M. C. Nussenzweig, mRNA vaccine-elicited antibodies to SARS-CoV-2 and circulating variants. *Nature* **592**, 616–622 (2021).
15. R. R. Goel, M. M. Painter, S. A. Apostolidis, D. Mathew, W. Meng, A. M. Rosenfeld, K. A. Lundgreen, A. Reynaldi, D. S. Khoury, A. Pattekar, S. Gouma, L. Kuri-Cervantes, P. Hicks, S. Dysinger, A. Hicks, H. Sharma, S. Herring, S. Korte, A. E. Baxter, D. A. Oldridge, J. R. Giles, M. E. Weirick, C. M. McAllister, M. Awofolaju, N. Tanenbaum, E. M. Drapeau, J. Dougherty, S. Long, K. D'Andrea, J. T. Hamilton, M. McLaughlin, J. C. Williams, S. Adamski, O. Kuthuru; UPenn COVID Processing Unit, I. Frank, M. R. Betts, L. A. Vella, A. Grifoni, D. Weiskopf, A. Sette, S. E. Hensley, M. P. Davenport, P. Bates, E. T. L. Prak, A. R. Greenplate, E. J. Wherry, S. Adamski, Z. Alam, M. M. Addison, K. T. Byrne, A. Chandra,

H. C. Descamps, N. Han, Y. Kaminskiy, S. C. Kammerman, J. Kim, A. R. Greenplate, J. T. Hamilton, N. Markosyan, J. H. Noll, D. K. Omran, A. Pattekar, E. Perkey, E. M. Prager, D. Pueschl, A. Rennels, J. B. Shah, J. S. Shilan, N. Wilhausen, A. N. Vanderbeck, mRNA vaccines induce durable immune memory to SARS-CoV-2 and variants of concern. *Science* , eabm0829 (2021).

16. V. Oberhardt, H. Luxenburger, J. Kemming, I. Schulien, K. Ciminski, S. Giese, B. Csernalabics, J. Lang-Meli, I. Janowska, J. Staniek, K. Wild, K. Basho, M. S. Marinescu, J. Fuchs, F. Topfstedt, A. Janda, O. Sogukpinar, H. Hilger, K. Stete, F. Emmerich, B. Bengsch, C. F. Waller, S. Rieg, Sagar, T. Boettler, K. Zoldan, G. Kochs, M. Schwemmle, M. Rizzi, R. Thimme, C. Neumann-Haefelin, M. Hofmann, Rapid and stable mobilization of $CD8^+$ T cells by SARS-CoV-2 mRNA vaccine. *Nature* **597**, 268–273 (2021).
17. M. M. Painter, D. Mathew, R. R. Goel, S. A. Apostolidis, A. Pattekar, O. Kuthuru, A. E. Baxter, R. S. Herati, D. A. Oldridge, S. Gouma, P. Hicks, S. Dysinger, K. A. Lundgreen, L. Kuri-Cervantes, S. Adamski, A. Hicks, S. Korte, J. R. Giles, M. E. Weirick, C. M. McAllister, J. Dougherty, S. Long, K. D'Andrea, J. T. Hamilton, M. R. Betts, P. Bates, S. E. Hensley, A. Grifoni, D. Weiskopf, A. Sette, A. R. Greenplate, E. J. Wherry, Rapid induction of antigen-specific $CD4^+$ T cells is associated with coordinated humoral and cellular immunity to SARS-CoV-2 mRNA vaccination. *Immunity* **54**, 2133–2142.e3 (2021).
18. P. S. Arunachalam, M. K. D. Scott, T. Hagan, C. Li, Y. Feng, F. Wimmers, L. Grigoryan, M. Trisal, V. V. Edara, L. Lai, S. E. Chang, A. Feng, S. Dhingra, M. Shah, A. S. Lee, S. Chinthrajah, S. B. Sindher, V. Mallajosyula, F. Gao, N. Sigal, S. Kowli, S. Gupta, K. Pellegrini, G. Tharp, S. Maysel-Auslender, S. Hamilton, H. Aoued, K. Hrusovsky, M. Roskey, S. E. Bosinger, H. T. Maecker, S. D. Boyd, M. M. Davis, P. J. Utz, M. S. Suthar, P. Khatri, K. C. Nadeau, B. Pulendran, Systems vaccinology of the BNT162b2 mRNA vaccine in humans. *Nature* **596**, 410–416 (2021).
19. K. S. Corbett, M. C. Nason, B. Flach, M. Gagne, S. O. Connell, T. S. Johnston, S. N. Shah, V. V. Edara, K. Floyd, L. Lai, C. McDanal, J. R. Francica, B. Flynn, K. Wu, A. Choi, M. Koch, O. M. Abiona, A. P. Werner, G. S. Alvarado, S. F. Andrew, M. M. Donaldson, J. Fintzi, D. R. Flebbe, E. Lamb, A. T. Noe, S. T. Nurmukhambetova, S. J. Provost, A. Cook, A. Dodson, A. Faudree, J. Greenhouse, S. Kar, L. Pessaint, M. Porto, K. Steingrebe, D. Valentin, S. Zouantcha, K. W. Bock, M. Minai, B. M. Nagata, J. I. Moliva, R. van de Wetering, S. Boyoglu-Barnum, K. Leung, W. Shi, E. S. Yang, Y. Zhang, J.-P. M. Todd, L. Wang, H. Andersen, K. E. Foulds, D. K. Edwards, J. R. Mascola, I. N. Moore, M. G. Lewis, A. Carfi, D. Montefiori, M. S. Suthar, A. McDermott, N. J. Sullivan, M. Roederer, D. C. Douek, B. S. Graham, R. A. Seder, Immune correlates of protection by mRNA-1273 immunization against SARS-CoV-2 infection in nonhuman primates. *Biorxiv Prepr Serv Biology* 2021.04.20.440647 (2021); https://doi.org/10.1101/2021.04.20.440647.
20. V. J. Hall, S. Foulkes, A. Charlett, A. Atti, E. J. M. Monk, R. Simmons, E. Wellington, M. J. Cole, A. Saei, B. Oguti, K. Munro, S. Wallace, P. D. Kirwan, M. Shrotri, A. Vusirikala, S. Rokadiya, M. Kall, M. Zambon, M. Ramsay, T. Brooks, C. S. Brown, M. A. Chand, S. Hopkins, N. Andrews, A. Atti, H. Aziz, T. Brooks, C. Brown, D. Camero, C. Carr, M. Chand, A. Charlett, H. Crawford, M. Cole, J. Conneely, S. D'Arcangelo, J. Ellis, S. Evans, S. Foulkes, N. Gillson, R. Gopal, L. Hall, V. Hall, P. Harrington, S. Hopkins, J. Hewson, K. Hoschler, D. Ironmonger, J. Islam, M. Kall, I. Karagiannis, O. Kay, J. Khawam, E. King, P. Kirwan, R. Kyffin, A. Lackenby, M. Lattimore, E. Linley, J. Lopez-Bernal, L. Mabey, R. McGregor, S. Miah, E. Monk, K. Munro, Z. Naheed, A. Nissr, A. O'Connell, B. Oguti, H. Okafor, S. Organ, J. Osbourne, A. Otter, M. Patel, S. Platt, D. Pople, K. Potts, M. Ramsay, J. Robotham, S. Rokadiya, C. Rowe, A. Saei, G. Sebbage, A. Semper, M. Shrotri, R. Simmons, A. Soriano, P. Staves, S. Taylor, A. Taylor, A. Tengbe, S. Tonge, A. Vusirikala, S. Wallace, E. Wellington, M. Zambon, D. Corrigan, M. Sartaj, L. Cromey, S. Campbell, K. Braithwaite, L. Price, L. Haahr, S. Stewart, E. Lacey, L. Partridge, G. Stevens, Y. Ellis, H. Hodgson, C. Norman, B. Larru, S. Mcwilliam, S. Winchester, P. Cieciwa, A. Pai, C. Loughrey, A. Watt, F. Adair, A. Hawkins, A. Grant, R. Temple-Purcell, J. Howard, N. Slawson, C. Subudhi, S. Davies, A. Bexley, R. Penn, N. Wong, G. Boyd, A. Rajgopal, A. Arenas-Pinto, R. Matthews, A. Whileman, R. Laugharne, J. Ledger, T. Barnes, C. Jones, D. Botes, N. Chitalia, S. Akhtar, G. Harrison, S. Horne, N. Walker, K. Agwuh, V. Maxwell, J. Graves, S. Williams, A. O'Kelly, P. Ridley, A. Cowley, H. Johnstone, P. Swift, J. Democratis, M. Meda, C. Callens, S. Beazer, S. Hams, V. Irvine, B. Chandrasekaran, C. Forsyth, J. Radmore, C. Thomas, K. Brown, S. Roberts, P. Burns, K. Gajee, T. Byrne, F. Sanderson, S. Knight, E. Macnaughton, B. Burton, H. Smith, R. Chaudhuri, K. Hollinshead, R. Shorten, A. Swan, R. Shorten, C. Favager, J. Murira, S. Baillon, S. Hamer, K. Gantert, J. Russell, D. Brennan, A. Dave, A. Chawla, F. Westell, D. Adeboyeku, P. Papineni, C. Pegg, M. Williams, S. Ahmad, S. Ingram, C. Gabriel, K. Pagget, P. Cieciwa, G. Maloney, J. Ashcroft, I. D. Rosario, R. Crosby-Nwaobi, C. Reeks, S. Fowler, L. Prentice, M. Spears, G. McKerron, K. McLelland-Brooks, J. Anderson, S. Donaldson, K. Templeton, L. Coke, N. Elumogo, J. Elliott, D. Padgett, A. Cross, J. Price, S. Joyce, I. Sinanovic, M. Howard, T. Lewis, P. Cowling, D. Potoczna, S. Brand, L. Sheridan, B. Wadams, A. Lloyd, J. Mouland, J. Giles, G. Pottinger, H. Coles, M. Joseph, M. Lee, S. Orr, H. Chenoweth, C. Auckland, R. Lear, T. Mahungu, A. Rodger, K. Penny-Thomas, S. Pai, J. Zamikula, E. Smith, S. Stone, E. Boldock, D. Howcroft, C. Thompson, M. Aga, P. Domingos, S. Gormley, C. Kerrison, L. Marsh, S. Tazzyman, L. Allsop, S. Ambalkar, M. Beekes, S. Jose, J. Tomlinson, A. Jones, C. Price, J. Pepperell, M. Schultz, J. Day, A. Boulos, E. Defever, D. McCracken, K. Brown, K. Gray, A. Houston, T. Planche, R. P. Jones, D. Wycherley, S. Bennett, J. Marrs, K. Nimako, B. Stewart, N. Kalakonda, S. Khanduri, A. Ashby, M. Holden, N. Mahabir, J. Harwood, B. Payne, K. Court, N. Staines, R. Longfellow, M. Green, L. Hughes, M. Halkes, P. Mercer, A. Roebuck, E. Wilson-Davies, L. Gallego, R. Lazarus, N. Aldridge, L. Berry, F. Game, T. Reynolds, C. Holmes, M. Wiselka, A. Higham, M. Booth, C. Duff, J. Alderton, H. Jory, E. Virgilio, T. Chin, M. Qazzafi, A. Moody, R. Tilley, T. Donaghy, K. Shipman, R. Sierra, N. Jones, G. Mills, D. Harvey, Y. Huang, J. Birch, L. Robinson, S. Board, A. Broadley, C. Laven, N. Todd, D. Eyre, K. Jeffery, S. Dunachie, C. Duncan, P. Klenerman, L. Turtle, H. Baxendale, J. Heeney, SARS-CoV-2 infection rates of antibody-positive compared with antibody-negative health-care workers in England: A large, multicentre, prospective cohort study (SIREN). *Lancet* **397**, 1459–1469 (2021).
21. D. S. Khoury, D. Cromer, A. Reynaldi, T. E. Schlub, A. K. Wheatley, J. A. Juno, K. Subbarao, S. J. Kent, J. A. Triccas, M. P. Davenport, Neutralizing antibody levels are highly predictive of immune protection from symptomatic SARS-CoV-2 infection. *Nat. Med.* **27**, 1205–1211 (2021).
22. I. Thevarajan, T. H. O. Nguyen, M. Koutsakos, J. Druce, L. Caly, C. E. van de Sandt, X. Jia, S. Nicholson, M. Catton, B. Cowie, S. Y. C. Tong, S. R. Lewin, K. Kedzierska, Breadth of concomitant immune responses prior to patient recovery: A case report of non-severe COVID-19. *Nat. Med.* **26**, 453–455 (2020).
23. D. Weiskopf, K. S. Schmitz, M. P. Raadsen, A. Grifoni, N. M. A. Okba, H. Endeman, J. P. C. van den Akker, R. Molenkamp, M. P. G. Koopmans, E. C. M. van Gorp, B. L. Haagmans, R. L. de Swart, A. Sette, R. D. de Vries, Phenotype and kinetics of SARS-CoV-2-specific T cells in COVID-19 patients with acute respiratory distress syndrome. *Sci. Immunol.* **5**, eabd2071 (2020).
24. T. Sekine, A. Perez-Potti, O. Rivera-Ballesteros, K. Strålin, J.-B. Gorin, A. Olsson, S. Llewellyn-Lacey, H. Kamal, G. Bogdanovic, S. Muschiol, D. J. Wullimann, T. Kammann, J. Emgård, T. Parrot, E. Folkesson; Karolinska COVID-19 Study Group, O. Rooyackers, L. I. Eriksson, J.-I. Henter, A. Sönnerborg, T. Allander, J. Albert, M. Nielsen, J. Klingström, S. Gredmark-Russ, N. K. Björkström, J. K. Sandberg, D. A. Price, H.-G. Ljunggren, S. Aleman, M. Buggert, Robust T cell immunity in convalescent individuals with asymptomatic or mild COVID-19. *Cell* **183**, 158–168.e14 (2020).
25. C. J. Reynolds, L. Swadling, J. M. Gibbons, C. Pade, M. P. Jensen, M. O. Diniz, N. M. Schmidt, D. K. Butler, O. E. Amin, S. N. L. Bailey, S. M. Murray, F. P. Pieper, S. Taylor, J. Jones, M. Jones, W.-Y. J. Lee, J. Rosenheim, A. Chandran, G. Joy, C. D. Genova, N. Temperton, J. Lambourne, T. Cutino-Moguel, M. Andiapen, M. Fontana, A. Smit, A. Semper, B. O'Brien, B. Chain, T. Brooks, C. Manisty, T. Treibel, J. C. Moon; COVIDsortium investigators, M. Noursadeghi; COVIDsortium immune correlates network, D. M. Altmann, M. K. Maini, Á. McKnight, R. J. Boyton, Discordant neutralizing antibody and T cell responses in asymptomatic and mild SARS-CoV-2 infection. *Sci. Immunol.* **5**, eabf3698 (2020).
26. L. B. Rodda, J. Netland, L. Shehata, K. B. Pruner, P. A. Morawski, C. D. Thouvenel, K. K. Takehara, J. Eggenberger, E. A. Hemann, H. R. Waterman, M. L. Fahning, Y. Chen, M. Hale, J. Rathe, C. Stokes, S. Wrenn, B. Fiala, L. Carter, J. A. Hamerman, N. P. King, M. Gale, D. J. Campbell, D. J. Rawlings, M. Pepper, Functional SARS-CoV-2-specific immune memory persists after mild COVID-19. *Cell* **184**, 169–183.e17 (2021).
27. A. K. Wheatley, J. A. Juno, J. J. Wang, K. J. Selva, A. Reynaldi, H.-X. Tan, W. S. Lee, K. M. Wragg, H. G. Kelly, R. Esterbauer, S. K. Davis, H. E. Kent, F. L. Mordant, T. E. Schlub, D. L. Gordon, D. S. Khoury, K. Subbarao, D. Cromer, T. P. Gordon, A. W. Chung, M. P. Davenport, S. J. Kent, Evolution of immune responses to SARS-CoV-2 in mild-moderate COVID-19. *Nat. Commun.* **12**, 1162 (2021).
28. C. K. Kang, M. Kim, S. Lee, G. Kim, P. G. Choe, W. B. Park, N. J. Kim, C.-H. Lee, I. S. Kim, K. Jung, D.-S. Lee, H. M. Shin, H.-R. Kim, M.-D. Oh, Longitudinal analysis of human memory T-cell response according to the severity of illness up to 8 months after SARS-CoV-2 infection. *J Infect Dis* **224**, 39–48 (2021).
29. S. Kalimuddin, C. Y. L. Tham, M. Qui, R. de Alwis, J. X. Y. Sim, J. M. E. Lim, H.-C. Tan, A. Syenina, S. L. Zhang, N. L. Bert, A. T. Tan, Y. S. Leong, J. X. Yee, E. Z. Ong, E. E. Ooi, A. Bertoletti, J. G. Low, Early T cell and binding antibody responses are associated with Covid-19 RNA vaccine efficacy onset. *Med* **2**, 682–688.e4 (2021).
30. B. A. Woldemeskel, C. C. Garliss, J. N. Blankson, SARS-CoV-2 mRNA vaccines induce broad CD4+ T cell responses that recognize SARS-CoV-2 variants and HCoV-NL63. *J. Clin. Invest.* **131**, e149335 (2021).
31. R. Hughes, L. Whitley, K. Fitovski, H.-M. Schneble, E. Muros, A. Sauter, L. Craveiro, P. Dillon, U. Bonati, N. Jessop, R. Pedotti, H. Koendgen, COVID-19 in ocrelizumab-treated people with multiple sclerosis. *Mult. Scler. Relat. Dis.* **49**, 102725 (2021).
32. P. Montero-Escribano, J. Matías-Guiu, P. Gómez-Iglesias, J. Porta-Etessam, V. Pytel, J. A. Matias-Guiu, Anti-CD20 and COVID-19 in multiple sclerosis and related disorders: A case series of 60 patients from Madrid, Spain. *Mult. Scler. Relat. Dis.* **42**, 102185 (2020).
33. K. A. Högelin, N. Ruffin, E. Pin, A. Månberg, S. Hober, G. Gafvelin, H. Grönlund, P. Nilsson, M. Khademi, T. Olsson, F. Piehl, F. A. Nimer, Development of humoral and cellular immunological memory against SARS-CoV-2 despite B-cell depleting treatment in multiple sclerosis. *iScience* **24**, 103078 (2021).

34. N. Dagan, N. Barda, E. Kepten, O. Miron, S. Perchik, M. A. Katz, M. A. Hernán, M. Lipsitch, B. Reis, R. D. Balicer, BNT162b2 mRNA Covid-19 vaccine in a nationwide mass vaccination setting. *New Engl. J. Med.* **384**, 1412–1423 (2021).
35. E. J. Haas, F. J. Angulo, J. M. McLaughlin, E. Anis, S. R. Singer, F. Khan, N. Brooks, M. Smaja, G. Mircus, K. Pan, J. Southern, D. L. Swerdlow, L. Jodar, Y. Levy, S. Alroy-Preis, Impact and effectiveness of mRNA BNT162b2 vaccine against SARS-CoV-2 infections and COVID-19 cases, hospitalisations, and deaths following a nationwide vaccination campaign in Israel: An observational study using national surveillance data. *Lancet* **397**, 1819–1829 (2021).
36. M. Bergwerk, T. Gonen, Y. Lustig, S. Amit, M. Lipsitch, C. Cohen, M. Mandelboim, E. G. Levin, C. Rubin, V. Indenbaum, I. Tal, M. Zavitan, N. Zuckerman, A. Bar-Chaim, Y. Kreiss, G. Regev-Yochay, Covid-19 breakthrough infections in vaccinated health care workers. *New Engl. J. Med.* **385**, 1474–1484 (2021).
37. T. Kustin, N. Harel, U. Finkel, S. Perchik, S. Harari, M. Tahor, I. Caspi, R. Levy, M. Leshchinsky, S. K. Dror, G. Bergerzon, H. Gadban, F. Gadban, E. Eliassian, O. Shimron, L. Saleh, H. Ben-Zvi, E. K. Taraday, D. Amichay, A. Ben-Dor, D. Sagas, M. Strauss, Y. S. Avni, A. Huppert, E. Kepten, R. D. Balicer, D. Netzer, S. Ben-Shachar, A. Stern, Evidence for increased breakthrough rates of SARS-CoV-2 variants of concern in BNT162b2-mRNA-vaccinated individuals. *Nat. Med.* **27**, 1379–1384 (2021).
38. E. G. Levin, Y. Lustig, C. Cohen, R. Fluss, V. Indenbaum, S. Amit, R. Doolman, K. Asraf, E. Mendelson, A. Ziv, C. Rubin, L. Freedman, Y. Kreiss, G. Regev-Yochay, Waning immune humoral response to BNT162b2 Covid-19 vaccine over 6 months. *New Engl. J. Med.* 10.1056/nejmoa2114583 (2021).
39. S. S. Ghorbani, N. Taherpour, S. Bayat, H. Ghajari, P. Mohseni, S. S. H. Nazari, Epidemiologic characteristics of cases with reinfection, recurrence, and hospital readmission due to COVID-19: A systematic review and meta-analysis. *J. Med. Virol.* **94**, 44–53 (2022).
40. A. T. Huang, B. Garcia-Carreras, M. D. T. Hitchings, B. Yang, L. C. Katzelnick, S. M. Rattigan, B. A. Borgert, C. A. Moreno, B. D. Solomon, L. Trimmer-Smith, V. Etienne, I. Rodriguez-Barraquer, J. Lessler, H. Salje, D. S. Burke, A. Wesolowski, D. A. T. Cummings, A systematic review of antibody mediated immunity to coronaviruses: Kinetics, correlates of protection, and association with severity. *Nat. Commun.* **11**, 4704 (2020).
41. W. J. Liu, M. Zhao, K. Liu, K. Xu, G. Wong, W. Tan, G. F. Gao, T-cell immunity of SARS-CoV: Implications for vaccine development against MERS-CoV. *Antiviral Res.* **137**, 82–92 (2017).
42. X. Guo, Z. Guo, C. Duan, Z. Chen, G. Wang, Y. Lu, M. Li, J. Lu, Long-term persistence of IgG antibodies in SARS-CoV infected healthcare workers. *Medrxiv*, 2020.02.12.20021386 (2020); https://doi.org/10.1101/2020.02.12.20021386.
43. H. Marcotte, A. Piralla, F. Zuo, L. Du, I. Cassaniti, H. Wan, M. Kumagai-Braesh, J. Andrell, E. Percivalle, J. C. Sammartino, Y. Wang, S. Vlachiotis, J. Attevall, F. Bergami, A. Ferrari, M. Colaneri, M. Vecchia, M. Sambo, V. Zuccaro, E. Asperges, R. Bruno, T. Oggionni, F. Meloni, H. Abolhassanni, F. Bertoglio, M. Schubert, L. Calzolai, L. Varani, M. Hust, Y. Xue, L. Hammarstrom, F. Baldanti, Q. Pan-Hammarstrom, Immunity to SARS-CoV-2 up to 15 months after infection. *bioRxiv* 2021.10.08.463699 (2021); https://doi.org/10.1101/2021.10.08.463699.
44. K. L. Flanagan, A. L. Fink, M. Plebanski, S. L. Klein, Sex and gender differences in the outcomes of vaccination over the life course. *Annu. Rev. Cell Dev. Biol.* **33**, 577–599 (2017).
45. R. R. Goel, S. A. Apostolidis, M. M. Painter, D. Mathew, A. Pattekar, O. Kuthuru, S. Gouma, P. Hicks, W. Meng, A. M. Rosenfeld, S. Dysinger, K. A. Lundgreen, L. Kuri-Cervantes, S. Adamski, A. Hicks, S. Korte, D. A. Oldridge, A. E. Baxter, J. R. Giles, M. E. Weirick, C. M. McAllister, J. Dougherty, S. Long, K. D'Andrea, J. T. Hamilton, M. R. Betts, E. T. L. Prak, P. Bates, S. E. Hensley, A. R. Greenplate, E. J. Wherry, Distinct antibody and memory B cell responses in SARS-CoV-2 naïve and recovered individuals following mRNA vaccination. *Sci. Immunol.* **6**, eabi6950 (2021).
46. K. A. Jabal, H. Ben-Amram, K. Beiruti, Y. Batheesh, C. Sussan, S. Zarka, M. Edelstein, Impact of age, ethnicity, sex and prior infection status on immunogenicity following a single dose of the BNT162b2 mRNA COVID-19 vaccine: Real-world evidence from healthcare workers, Israel, December 2020 to January 2021. *Eurosurveillance* **26**, 2100096 (2021).
47. D. A. Collier, I. A. T. M. Ferreira, P. Kotagiri, R. Datir, E. Lim, E. Touizer, B. Meng, A. Abdullahi; The CITIID-NIHR BioResource COVID-19 Collaboration, A. Elmer, N. Kingston, B. Graves, E. L. Gresley, D. Caputo, L. Bergamaschi, K. G. C. Smith, J. R. Bradley, L. Ceron-Gutierrez, P. Cortes-Acevedo, G. Barcenas-Morales, M. A. Linterman, L. E. Mc Coy, C. Davis, E. Thomson, P. A. Lyons, E. M. Kinney, R. Doffinger, M. Wills, R. K. Gupta, Age-related immune response heterogeneity to SARS-CoV-2 vaccine BNT162b2. *Nature* **596**, 417–422 (2021).
48. S. Reiss, A. E. Baxter, K. M. Cirelli, J. M. Dan, A. Morou, A. Daigneault, N. Brassard, G. Silvestri, J.-P. Routy, C. Havenar-Daughton, S. Crotty, D. E. Kaufmann, Comparative analysis of activation induced marker (AIM) assays for sensitive identification of antigen-specific CD4 T cells. *PLOS ONE* **12**, e0186998 (2017).
49. L. Loyal, J. Braun, L. Henze, B. Kruse, M. Dingeldey, U. Reimer, F. Kern, T. Schwarz, M. Mangold, C. Unger, F. Dörfler, S. Kadler, J. Rosowski, K. Gürcan, Z. Uyar-Aydin, M. Frentsch, F. Kurth, K. Schnatbaum, M. Eckey, S. Hippenstiel, A. Hocke, M. A. Müller, B. Sawitzki, S. Miltenyi, F. Paul, M. A. Mall, H. Wenschuh, S. Voigt, C. Drosten, R. Lauster, N. Lachman, L.-E. Sander, V. M. Corman, J. Röhmel, L. Meyer-Arndt, A. Thiel, C. Giesecke-Thiel, Cross-reactive $CD4^+$ T cells enhance SARS-CoV-2 immune responses upon infection and vaccination. *Science* **374**, eabh1823 (2021).
50. L. Gattinoni, D. E. Speiser, M. Lichterfeld, C. Bonini, T memory stem cells in health and disease. *Nat. Med.* **23**, 18–27 (2017).
51. L. Gattinoni, E. Lugli, Y. Ji, Z. Pos, C. M. Paulos, M. F. Quigley, J. R. Almeida, E. Gostick, Z. Yu, C. Carpenito, E. Wang, D. C. Douek, D. A. Price, C. H. June, F. M. Marincola, M. Roederer, N. P. Restifo, A human memory T cell subset with stem cell–like properties. *Nat. Med.* **17**, 1290–1297 (2011).
52. J. Braun, L. Loyal, M. Frentsch, D. Wendisch, P. Georg, F. Kurth, S. Hippenstiel, M. Dingeldey, B. Kruse, F. Fauchere, E. Baysal, M. Mangold, L. Henze, R. Lauster, M. A. Mall, K. Beyer, J. Röhmel, S. Voigt, J. Schmitz, S. Miltenyi, I. Demuth, M. A. Müller, A. Hocke, M. Witzenrath, N. Suttorp, F. Kern, U. Reimer, H. Wenschuh, C. Drosten, V. M. Corman, C. Giesecke-Thiel, L. E. Sander, A. Thiel, SARS-CoV-2-reactive T cells in healthy donors and patients with COVID-19. *Nature* **587**, 270–274 (2020).
53. J. Mateus, A. Grifoni, A. Tarke, J. Sidney, S. I. Ramirez, J. M. Dan, Z. C. Burger, S. A. Rawlings, D. M. Smith, E. Phillips, S. Mallal, M. Lammers, P. Rubiro, L. Quiambao, A. Sutherland, E. D. Yu, R. da Silva Antunes Antunes, J. Greenbaum, A. Frazier, A. J. Markmann, L. Premkumar, A. de Silva, B. Peters, S. Crotty, A. Sette, D. Weiskopf, Selective and cross-reactive SARS-CoV-2 T cell epitopes in unexposed humans. *Science* **370**, 89–94 (2020).
54. P. Bacher, E. Rosati, D. Esser, G. R. Martini, C. Saggau, E. Schiminsky, J. Dargvainiene, I. Schröder, I. Wieters, Y. Khodamoradi, F. Eberhardt, M. J. G. T. Vehreschild, H. Neb, M. Sonntagbauer, C. Conrad, F. Tran, P. Rosenstiel, R. Markewitz, K.-P. Wandinger, M. Augustin, J. Rybniker, M. Kochanek, F. Leypoldt, O. A. Cornely, P. Koehler, A. Franke, A. Scheffold, Low-avidity $CD4^+$ T cell responses to SARS-CoV-2 in unexposed individuals and humans with severe COVID-19. *Immunity* **53**, 1258–1271.e5 (2020).
55. S. Crotty, A brief history of T cell help to B cells. *Nat. Rev. Immunol.* **15**, 185–189 (2015).
56. R. S. Herati, M. A. Reuter, D. V. Dolfi, K. D. Mansfield, H. Aung, O. Z. Badwan, R. K. Kurupati, S. Kannan, H. Ertl, K. E. Schmader, M. R. Betts, D. H. Canaday, E. J. Wherry, Circulating CXCR5+PD-1+ response predicts influenza vaccine antibody responses in young adults but not elderly adults. *J. Immunol.* **193**, 3528–3537 (2014).
57. S.-E. Bentebibel, S. Lopez, G. Obermoser, N. Schmitt, C. Mueller, C. Harrod, E. Flano, A. Mejias, R. A. Albrecht, D. Blankenship, H. Xu, V. Pascual, J. Banchereau, A. Garcia-Sastre, A. K. Palucka, O. Ramilo, H. Ueno, Induction of $ICOS^+CXCR3^+CXCR5^+$ T_H cells correlates with antibody responses to influenza vaccination. *Sci. Transl. Med.* **5**, 176ra32 (2013).
58. N. Kaneko, H.-H. Kuo, J. Boucau, J. R. Farmer, H. Allard-Chamard, V. S. Mahajan, A. Piechocka-Trocha, K. Lefteri, M. Osborn, J. Bals, Y. C. Bartsch, N. Bonheur, T. M. Caradonna, J. Chevalier, F. Chowdhury, T. J. Diefenbach, K. Einkauf, J. Fallon, J. Feldman, K. K. Finn, P. Garcia-Broncano, C. A. Hartana, B. M. Hauser, C. Jiang, P. Kaplonek, M. Karpell, E. C. Koscher, X. Lian, H. Liu, J. Liu, N. L. Ly, A. R. Michell, Y. Rassadkina, K. Seiger, L. Sessa, S. Shin, N. Singh, W. Sun, X. Sun, H. J. Ticheli, M. T. Waring, A. L. Zhu, G. Alter, J. Z. Li, D. Lingwood, A. G. Schmidt, M. Lichterfeld, B. D. Walker, X. G. Yu, R. F. Padera, S. Pillai; the Massachusetts Consortium on Pathogen Readiness Specimen Working Group, Loss of Bcl-6-expressing T follicular helper cells and germinal centers in COVID-19. *Cell* **183**, 143–157.e13 (2020).
59. J. S. Turner, J. A. O'Halloran, E. Kalaidina, W. Kim, A. J. Schmitz, J. Q. Zhou, T. Lei, M. Thapa, R. E. Chen, J. B. Case, F. Amanat, A. M. Rauseo, A. Haile, X. Xie, M. K. Klebert, T. Suessen, W. D. Middleton, P.-Y. Shi, F. Krammer, S. A. Teefey, M. S. Diamond, R. M. Presti, A. H. Ellebedy, SARS-CoV-2 mRNA vaccines induce persistent human germinal centre responses. *Nature* **596**, 109–113 (2021).
60. K. Lederer, K. Parvathaneni, M. M. Painter, E. Bettini, D. Agarwal, K. A. Lundgreen, M. Weirick, R. R. Goel, X. Xu, E. M. Drapeau, S. Gouma, A. R. Greenplate, C. L. Coz, N. Romberg, L. Jones, M. Rosen, B. Besharatian, M. Kaminiski, D. Weiskopf, A. Sette, S. E. Hensley, P. Bates, E. J. Wherry, A. Naji, V. Bhoj, M. Locci, Germinal center responses to SARS-CoV-2 mRNA vaccines in healthy and immunocompromised individuals. *Medrxiv*, 2021.09.16.21263686 (2021); https://doi.org/10.1101/2021.09.16.21263686.
61. K. A. Fraser, J. M. Schenkel, S. C. Jameson, V. Vezys, D. Masopust, Preexisting high frequencies of memory CD8+ T cells favor rapid memory differentiation and preservation of proliferative potential upon boosting. *Immunity* **39**, 171–183 (2013).
62. A. L. Cunningham, T. C. Heineman, H. Lal, O. Godeaux, R. Chlibek, S.-J. Hwang, J. E. McElhaney, T. Vesikari, C. Andrews, W. S. Choi, M. Esen, H. Ikematsu, M. K. Choma, K. Pauksens, S. Ravault, B. Salaun, T. F. Schwarz, J. Smetana, C. V. Abeele, P. V. den Steen, I. Vastiau, L. Y. Weckx, M. J. Levin; ZOE-50/70 Study Group, Immune responses to a recombinant glycoprotein E herpes zoster vaccine in adults aged 50 years or older. *J Infect Dis* **217**, 1750–1760 (2018).
63. P. A. Darrah, D. T. Patel, P. M. D. Luca, R. W. B. Lindsay, D. F. Davey, B. J. Flynn, S. T. Hoff, P. Andersen, S. G. Reed, S. L. Morris, M. Roederer, R. A. Seder, Multifunctional TH1 cells define a correlate of vaccine-mediated protection against Leishmania major. *Nat. Med.* **13**, 843–850 (2007).
64. M. H. G. Pereira, M. M. Figueiredo, C. P. Queiroz, T. V. B. Magalhães, A. Mafra, L. M. O. Diniz, Ú. L. Costa, K. J. Gollob, L. R. do Valle Antonelli, H. da Costa Santiago, T-cells producing

multiple combinations of IFNγ, TNF and IL10 are associated with mild forms of dengue infection. *Immunology* **160**, 90–102 (2020).
65. M. Wilkie, I. Satti, A. Minhinnick, S. Harris, M. Riste, R. L. Ramon, S. Sheehan, Z.-R. M. Thomas, D. Wright, L. Stockdale, A. Hamidi, M. K. O'Shea, K. Dwivedi, H. M. Behrens, T. Davenne, J. Morton, S. Vermaak, A. Lawrie, P. Moss, H. McShane, A phase I trial evaluating the safety and immunogenicity of a candidate tuberculosis vaccination regimen, ChAdOx1 85A prime—MVA85A boost in healthy UK adults. *Vaccine* **38**, 779–789 (2020).
66. M. L. Precopio, M. R. Betts, J. Parrino, D. A. Price, E. Gostick, D. R. Ambrozak, T. E. Asher, D. C. Douek, A. Harari, G. Pantaleo, R. Bailer, B. S. Graham, M. Roederer, R. A. Koup, Immunization with vaccinia virus induces polyfunctional and phenotypically distinctive $CD8^+$ T cell responses. *J. Exp. Med.* **204**, 1405–1416 (2007).
67. T. D. Querec, R. S. Akondy, E. K. Lee, W. Cao, H. I. Nakaya, D. Teuwen, A. Pirani, K. Gernert, J. Deng, B. Marzolf, K. Kennedy, H. Wu, S. Bennouna, H. Oluoch, J. Miller, R. Z. Vencio, M. Mulligan, A. Aderem, R. Ahmed, B. Pulendran, Systems biology approach predicts immunogenicity of the yellow fever vaccine in humans. *Nat. Immunol.* **10**, 116–125 (2009).
68. D. Gaucher, R. Therrien, N. Kettaf, B. R. Angermann, G. Boucher, A. Filali-Mouhim, J. M. Moser, R. S. Mehta, D. R. Drake, E. Castro, R. Akondy, A. Rinfret, B. Yassine-Diab, E. A. Said, Y. Chouikh, M. J. Cameron, R. Clum, D. Kelvin, R. Somogyi, L. D. Greller, R. S. Balderas, P. Wilkinson, G. Pantaleo, J. Tartaglia, E. K. Haddad, R.-P. Sékaly, Yellow fever vaccine induces integrated multilineage and polyfunctional immune responses. *J. Exp. Med.* **205**, 3119–3131 (2008).
69. S. Sridhar, S. Begom, A. Bermingham, K. Hoschler, W. Adamson, W. Carman, T. Bean, W. Barclay, J. J. Deeks, A. Lalvani, Cellular immune correlates of protection against symptomatic pandemic influenza. *Nat. Med.* **19**, 1305–1312 (2013).
70. R. R. Goel, M. M. Painter, S. A. Apostolidis, D. Mathew, W. Meng, A. M. Rosenfeld, K. A. Lundgreen, A. Reynaldi, D. S. Khoury, A. Pattekar, S. Gouma, L. Kuri-Cervantes, P. Hicks, S. Dysinger, A. Hicks, H. Sharma, S. Herring, S. Korte, A. E. Baxter, D. A. Oldridge, J. R. Giles, M. E. Weirick, C. M. McAllister, M. Awofolaju, N. Tanenbaum, E. M. Drapeau, J. Dougherty, S. Long, K. D'Andrea, J. T. Hamilton, M. McLaughlin, J. C. Williams, S. Adamski, O. Kuthuru; UPenn COVID Processing Unit, I. Frank, M. R. Betts, L. A. Vella, A. Grifoni, D. Weiskopf, A. Sette, S. E. Hensley, M. P. Davenport, P. Bates, E. T. L. Prak, A. R. Greenplate, E. J. Wherry, mRNA vaccination induces durable immune memory to SARS-CoV-2 with continued evolution to variants of concern.*bioRxiv*, 2021.08.23.457229 (2021).
71. J. Liu, Y. Liu, H. Xia, J. Zou, S. C. Weaver, K. A. Swanson, H. Cai, M. Cutler, D. Cooper, A. Muik, K. U. Jansen, U. Sahin, X. Xie, P. R. Dormitzer, P.-Y. Shi, BNT162b2-elicited neutralization of B.1.617 and other SARS-CoV-2 variants. *Nature* **596**, 273–275 (2021).
72. H. G. Rammensee, K. Falk, O. Rötzschke, Peptides naturally presented by MHC class I molecules. *Annu. Rev. Immunol.* **11**, 213–244 (1993).
73. J. D. Miller, R. G. van der Most, R. S. Akondy, J. T. Glidewell, S. Albott, D. Masopust, K. Murali-Krishna, P. L. Mahar, S. Edupuganti, S. Lalor, S. Germon, C. D. Rio, M. J. Mulligan, S. I. Staprans, J. D. Altman, M. B. Feinberg, R. Ahmed, Human effector and memory $CD8^+$ T cell responses to smallpox and yellow fever vaccines. *Immunity* **28**, 710–722 (2008).
74. P. C. del Amo, J. L. Beneytez, L. Boelen, R. Ahmed, K. L. Miners, Y. Zhang, L. Roger, R. E. Jones, S. A. F. Marraco, D. E. Speiser, D. M. Baird, D. A. Price, K. Ladell, D. Macallan, B. Asquith, Human T_{SCM} cell dynamics in vivo are compatible with long-lived immunological memory and stemness. *PLoS Biol.* **16**, e2005523 (2018).
75. R. S. Akondy, M. Fitch, S. Edupuganti, S. Yang, H. T. Kissick, K. W. Li, B. A. Youngblood, H. A. Abdelsamed, D. J. McGuire, K. W. Cohen, G. Alexe, S. Nagar, M. M. McCausland, S. Gupta, P. Tata, W. N. Haining, M. J. McElrath, D. Zhang, B. Hu, W. J. Greenleaf, J. J. Goronzy, M. J. Mulligan, M. Hellerstein, R. Ahmed, Origin and differentiation of human memory CD8 T cells after vaccination. *Nature* **552**, 362–367 (2017).
76. S. A. F. Marraco, C. Soneson, L. Cagnon, P. O. Gannon, M. Allard, S. A. Maillard, N. Montandon, N. Rufer, S. Waldvogel, M. Delorenzi, D. E. Speiser, Long-lasting stem cell–like memory $CD8^+$ T cells with a naïve-like profile upon yellow fever vaccination. *Sci. Transl. Med.* **7**, 282ra48 (2015).
77. S. L. Klein, K. L. Flanagan, Sex differences in immune responses. *Nat. Rev. Immunol.* **16**, 626–638 (2016).
78. C. Gebhard, V. Regitz-Zagrosek, H. K. Neuhauser, R. Morgan, S. L. Klein, Impact of sex and gender on COVID-19 outcomes in Europe. *Biol. Sex Differ.* **11**, 29 (2020).
79. S. Y. Tartof, J. M. Slezak, H. Fischer, V. Hong, B. K. Ackerson, O. N. Ranasinghe, T. B. Frankland, O. A. Ogun, J. M. Zamparo, S. Gray, S. R. Valluri, K. Pan, F. J. Angulo, L. Jodar, J. M. McLaughlin, Effectiveness of mRNA BNT162b2 COVID-19 vaccine up to 6 months in a large integrated health system in the USA: A retrospective cohort study. *Lancet* **398**, 1407–1416 (2021).
80. J. L. Bernal, N. Andrews, C. Gower, E. Gallagher, R. Simmons, S. Thelwall, J. Stowe, E. Tessier, N. Groves, G. Dabrera, R. Myers, C. N. J. Campbell, G. Amirthalingam, M. Edmunds, M. Zambon, K. E. Brown, S. Hopkins, M. Chand, M. Ramsay, Effectiveness of Covid-19 Vaccines against the B.1.617.2 (Delta) Variant. *New Engl. J. Med.* **385**, 585–594 (2021).
81. H. Chemaitelly, P. Tang, M. R. Hasan, S. AlMukdad, H. M. Yassine, F. M. Benslimane, H. A. A. Khatib, P. Coyle, H. H. Ayoub, Z. A. Kanaani, E. A. Kuwari, A. Jeremijenko, A. H. Kaleeckal, A. N. Latif, R. M. Shaik, H. F. A. Rahim, G. K. Nasrallah, M. G. A. Kuwari, H. E. A. Romaihi, A. A. Butt, M. H. Al-Thani, A. A. Khal, R. Bertollini, L. J. Abu-Raddad, Waning of BNT162b2 vaccine protection against SARS-CoV-2 infection in Qatar. *New Engl. J. Med.*, 10.1056/nejmoa2114114 (2021).
82. K. Lederer, D. Castaño, D. G. Atria, T. H. Oguin, S. Wang, T. B. Manzoni, H. Muramatsu, M. J. Hogan, F. Amanat, P. Cherubin, K. A. Lundgreen, Y. K. Tam, S. H. Y. Fan, L. C. Eisenlohr, I. Maillard, D. Weissman, P. Bates, F. Krammer, G. D. Sempowski, N. Pardi, M. Locci, SARS-CoV-2 mRNA vaccines foster potent antigen-specific germinal center responses associated with neutralizing antibody generation. *Immunity* **53**, 1281–1295.e5 (2020).
83. A. Tarke, J. Sidney, N. Methot, E. D. Yu, Y. Zhang, J. M. Dan, B. Goodwin, P. Rubiro, A. Sutherland, E. Wang, A. Frazier, S. I. Ramirez, S. A. Rawlings, D. M. Smith, R. da Silva Antunes, B. Peters, R. H. Scheuermann, D. Weiskopf, S. Crotty, A. Grifoni, A. Sette, Impact of SARS-CoV-2 variants on the total $CD4^+$ and $CD8^+$ T cell reactivity in infected or vaccinated individuals. *Cell Rep. Med.* **2**, 100355 (2021).
84. Strategies for Management of Antiretroviral Therapy (SMART) Study Group, W. M. El-Sadr, J. D. Lundgren, J. D. Neaton, F. Gordin, D. Abrams, R. C. Arduino, A. Babiker, W. Burman, N. Clumeck, C. J. Cohen, D. Cohn, D. Cooper, J. Darbyshire, S. Emery, G. Fätkenheuer, B. Gazzard, B. Grund, J. Hoy, K. Klingman, M. Losso, N. Markowitz, J. Neuhaus, A. Phillips, C. Rappoport, $CD4^+$ count–guided interruption of antiretroviral treatment. *New Engl. J. Med.* **355**, 2283–2296 (2006).
85. C. Strafella, V. Caputo, G. Guerrera, A. Termine, C. Fabrizio, R. Cascella, M. Picozza, C. Caltagirone, A. Rossini, M. P. Balice, A. Salvia, L. Battistini, G. Borsellino, E. Giardina, Case report: Sars-CoV-2 infection in a vaccinated individual: Evaluation of the immunological profile and virus transmission risk. *Front. Immunol.* **12**, 708820 (2021).
86. M. Roederer, J. L. Nozzi, M. C. Nason, SPICE: Exploration and analysis of post-cytometric complex multivariate datasets. *Cytometry A* **79**, 167–174 (2011).

Acknowledgments: We thank the volunteers for donating their blood and time, and the nurses for their assistance. We are grateful to D. F. Angelini for critically reading the manuscript and to L. De Marco for data reanalysis and help with the figures. **Funding:** This work was partially supported by a grant of the Italian Ministry of Health to L.B. (COVID-2020-12371735).
Author contributions: G.B., L.B., and A.R. conceptualized the study. A.R., A.S., and C.C. performed vaccination supervision and donor enrollment. G.G., R.P., S.D., A.V., M. Pirronello, M.S., and F.G. performed cell stimulations, stainings, flow cytometry experiments, and cytokine measurements. M.P.B. performed antibody dosage. G.B. prepared the dataset for analysis. G.B. and M. Picozza performed descriptive statistics. A.T. and C.F. did the statistical analysis. Funding acquisition: L.B. Writing—original draft: G.B. Writing—review and editing: G.B., M. Picozza, and L.B., with input from all authors. **Competing interests:** The authors declare that they have no competing interests. **Data and materials availability:** All data needed to evaluate the conclusions in the paper are present in the paper or the Supplementary Materials.

Submitted 27 September 2021
Accepted 28 October 2021
Published 24 December 2021
10.1126/sciimmunol.abl5344